Dear editor Peter Haynes,

We thank the referees for the helpful comments which helped to improve the manuscript significantly. We are particularly grateful for the suggestions about the hydrostatic adjustment mechanism, which clarifies our results in section 3.2. Also, we included a new section 4.3 to discuss how much of the TIL is left without the equatorial wave signal, other mechanisms that could enhance the remaining TIL, and the forcing of the secondary N^2 maximum. We find that this new subsection puts our results in a better context and makes the paper rounder as a whole.

Please find the revised manuscript with highlighted changes in the supplement, and the point-by-point responses to the referees comments as individual replies. We hope the new version of the manuscript fulfills the referees' requests.

Yours sincerely,

Robin Pilch Kedzierski
Katja Matthes
Karl Bumke

Response to Referee #1

We thank Referee #1 for the helpful comments which helped to improve the manuscript significantly.

In the following, we first explain general changes made in the manuscript, and continue with the point-by-point responses to the reviewer's comments. The referee's comments are in blue font, and our replies are in normal font. Every change made in the revised manuscript is highlighted (please find the highlighted version in the Author Response).

General comments:

New subsection 4.3 and Figure 7

Motivated by the specific comments 2 and 3 by Joowan Kim in his review, we added subsection 4.3 to the manuscript in order to discuss how much of the TIL is left without the equatorial wave signal, other mechanisms that could enhance the remaining TIL, and the forcing of the secondary N^2 maximum. Figure 7 compares the time evolution of the equatorial N^2 structure with and without the equatorial wave signal (Thomas Birner asked about this during the SHARP2016 workshop, and we found that making this kind of plot would be the best fit for the purposes of section 4.3).

In Fig. 7 the difference in the TIL region when the equatorial wave signal is subtracted is clear, but the secondary N^2 maximum below the descending westerly QBO phase remains the same, and therefore is not directly modulated by Kelvin waves, as we were suggesting in the discussion manuscript version. Since proven untrue, the paragraphs that discussed the forcing of the secondary N^2 maximum by the filtered Kelvin waves have been erased (now missing from lines 368, 403, 479 and 563), and now we discuss possible forcings in lines 518-527. We still suggest an indirect effect of Kelvin waves (T signal from wave dissipation), but this cannot be captured by our wavenumber-frequency domain filters once the wave dissipates.

New Appendix C

We added a caveat about the filtering of waves with periods of less than 2 days from our daily dataset. Spectral ringing can be an issue with these settings, and could leave a spurious signal in our results (Figure 6), but we checked that the contribution of these periods to the calculated equatorial wave signature of inertia-gravity waves is zero, and therefore doesn't affect our results at all.

Point-by-point responses to Ref#1 comments

Major issues

1. I am not an expert on reanalysis data, but as far as I know the quality of reanalysis wind data in the tropics is not as good as one would wish them to be. So the question is: how much can you trust the upper tropospheric horizontal divergence in the tropics? The authors should at least address this issue and try to convince the reader that the quality of the data is sufficient for their purpose.

We agree in that upper-tropospheric winds in ERA-Interim in the tropics are somewhat less accurate than in the extratropics, but we don't think the difference is enough to make tropical 100hPa divergence unreliable for the following reasons:

1) Globally, the performance of ERA-Interim at the 100hPa level is comparable to the operational weather forecast system from ECMWF in terms of root mean squared (RMS) error relative to radiosondes (see Figure 1a from Dee et al., 2011). Note that this figure compares RMS of ERA-Interim 1979 analyses (well before GPS-RO was available), to RMS in operational forecasts in 2007. The 100hPa level in ERA-Interim is as good as one can get from state-of-the-art NWP systems.

2) In the extratropics, the wind difference between in-situ observations and ERA-Interim reanalysis has a 1 standard deviation of about 3m/s for both zonal and meridional winds. In the tropics, this difference at 100hPa is of about 4m/s, meaning that the extratropics have about 75% of the inaccuracy found in tropical upper-tropospheric winds (see Figures 17 and 18 from Poli et al., 2010). Also, the tropical winds at 100hPa don't have the worst performance, since the levels between 120-200hPa in the tropics have a higher 1std difference of 4.5m/s. In addition, the assimilation of GPS-RO observations slightly reduces this differences about everywhere.

3) In-situ observations, radiosondes, have uncertainties as well: several m/s of standard error can be observed applying different tracking techniques, and the errors highly depend on the wind regime, shear and rate of vertical ascent. Also, high-resolution radiosondes include small-scale variations of winds (also up to a few m/s) that cannot be resolved by the model's vertical grid. A thorough description of these issues with wind observations can be found at the "GUIDE TO METEOROLOGICAL INSTRUMENTS AND METHODS OF OBSERVATION" (WMO-No. 8), Part I, chapter 13.

We feel there is no need to discuss this issue in the manuscript, but we added a short sentence in lines 102-104 about it.

2. The authors could clarify the role of tropospheric vertical motion and upper tropospheric horizontal divergence for tropical TIL formation, e.g. in their section 3.2. Assuming that a tropospheric wave produces regional upwelling with horizontal divergence right at the tropopause level, this would yield a higher and sharper than normal tropopause (corresponding to a stronger than normal TIL) — essentially by pushing upward the tropopause and thereby making the lowermost stratosphere somewhat colder. In this simple scenario there is no warming involved at any point: the TIL forms because the cooling has some vertical structure decaying with altitude. On the other hand, composite plots like Figure 6a indicate actually some warming in the lowermost stratosphere. Does this mean that the equatorial waves are associated with downwelling in the lowermost stratosphere (right above the tropospheric upwelling), or does this possibly imply diabatic warming?

Regarding divergence, we connect it to convection and tropopause cooling by the hydrostatic adjustment mechanism. Here the suggestions of Joowan Kim were helpful in providing references for a clearer explanation for the sharper TIL with divergent flow (see specific comment 3 of his review). It has to be noted that this mechanism and our results with divergence from Figures 2 and 3 are independent of equatorial wave activity: deep convection (and near-tropopause divergence) can be coupled to an equatorial wave or not, and is represented either way in the diagram of sTIL versus divergence in Fig. 3. We added a new paragraph discussing this within section 3.2, lines 300-307.

The equatorial wave signature in Figure 6a comes entirely from making a tropopause-based mean of the different wave anomalies: it appears because the tropopause is adjusted to the wave anomalies – a ground based mean gives zero. The reason for this is that a Fast Fourier Transform separates a field into a sum of harmonics, which are deviations from the zonal mean. The constant (ground-based zonal mean) term is not included in the wave signals obtained by the filtering method, and the ground-based sum of the positive-negative parts of each harmonic is zero. It is the tropopause undulations and the tropopause-based averaging that enable the signature in Fig. 6a to appear, and we make this clear throughout section 4.2 now.

Our method is suited to compare the signal of the different equatorial wave types on the TIL: therefore the tropopause-based averaging of the temperature and N^2 profiles while creating a gridded dataset, and the tropopause-based averaging of the wave anomalies.

However, conclusions about vertical motion cannot be inferred from Figure 6: the observations we work with are temperatures from GPS-RO and the filtered wave anomalies, and vertical motion is a derived, indirect quantity that can be obtained from models, whose vertical resolution is not enough to enable a study of the relation of upwelling and the small-scale filtered anomalies.

In a scenario of zonal-mean ascent in the upper troposphere, a wave would consist of a harmonic of upwelling and downwelling *anomalies* from this zonal mean*:* there would be a local cooling effect (to which the tropopause would be lifted by the extra upwelling, therefore adjusting to the anomaly), and a local warm anomaly somewhere else, which would fall above the tropopause since it's not necessarily been lifted there. Thus, the tropopause-based zonal mean would show the dipole of tropopause cooling and warming aloft. Once the wave has a vertical phase tilt (a more realistic scenario, e.g. Figure 5a) this dipole can be present in the same place, otherwise the cooling/warming are in different regions. The warm anomaly doesn't imply downwelling per se, it may as well be less upwelling. In this scenario, the existence of the wave doesn't affect the zonal-mean ascent: only the tropopause horizontal structure and the TIL. Non-linear interactions are needed for a wave to change the zonal-mean flow (e.g. wave breaking), these can be complex and are beyond the scope of our study.

Our method and corresponding results in section 4 were specifically designed to target TIL forcing, and they don't give conclusions about vertical motion related to equatorial wave activity. In section 3.2, divergence is related to vertical wind convergence, which doesn't give information about the actual rate of ascent, just its gradient at that level independently of wave activity. For these reasons, we find that a discussion about vertical motion in sections 3.2 and 4 is very difficult to link to our results while not adding insight about the TIL.

Minor issues

1. Line 166: What is an e-fold function? A Gaussian?

We renamed the function into 'exponentially-folding' (l. 169) for better clarity. Note that the mathematical expression of the weighting function is in line 171.

2. Line 172: How are the profiles shifted in altitude? By how much? For what purpose?

The profiles are shifted from a tropopause-based scale onto a ground-based one. We rephrased lines 175-176 to clarify this. The purpose of making tropopause-based averages while gridding GPS-RO profiles is to smooth the TIL as little as possible (l. 190). The filtering has to be done at ground-based levels, since we know the tropopause undulates, adjusts to the equatorial wave signal and is not a constant reference level.

3. If I recall right, an important point in the work of Wheeler and Kiladis (1999) is the removal of the background spectrum. How is this dealt with in the present work?

In Wheeler and Kiladis (1999) the background power spectrum is calculated to discern which regions of the wavenumber-frequency domain have a spectral signature significantly above the background (Fig. 3 of their paper). We don't present such diagrams in our study. While filtering, the inclusion of background noise is unavoidable, but it appears as a continuum of small amplitude fluctuations: please see the beginning of section 4 in Wheeler and Kiladis (1999). The background spectrum doesn't need to be removed since the filtered wave anomalies appear as bursts of high amplitude compared to it.

4. As a standard reference for the seasonal cycle of the tropical tropopause one should add the paper by Yulaeva et al. (1994).

Agreed, this reference was added in line 229.

5. Line 258, ".... temperature inversion is added to this background profile...": For me, "temperature inversion" means that the temperature increases (rather than decreases) with altitude. It seems that this term should only be used for full temperature profiles, not for perturbations or "additions". So I have a difficulty with the expression "adding a temperature inversion to the background profile".

We changed the term 'temperature inversion' for 'dipole of tropopause cooling and warming aloft' in the sentence, see l. 265.

6. Line 259: "skyrocket" appears too colloquial and not quite fitting here.

We changed this term for 'increases dramatically' in the sentence, see l.266.

7. Line 260, "the N^2_{max} is very narrow": strictly speaking this is not true. The peak containing N^2_{max} may be very narrow, not the N^2_{max} itself.

Agreed, the sentence was changed accordingly (see l. 268).

8. Line 336: How is the significance of the difference between the curves assessed? As far as I know, the significance of the difference in the mean between two distributions is measured by the standard error (Press et al., 1992), not by the standard deviation.

The purpose of the sentence was to infer that a significance test is not needed: the two means are separated by 30 standard deviations, which is really far apart. A common way to assess the significance of the difference in the mean of two distributions is a t-test. The difference between the

Easterly-Westerly QBO N^2_{max} distributions is well beyond the 99.9% significance level, as we now explain in lines 356-359. We prefer not to use the term 'standard error' since both distributions are true.

9. Line 364: How was the longitude chosen for the plots in figure 5?

We found that the word 'sections' might have been misleading in the sentence. We changed it for 'snapshots' (l. 380 now). There is no longitude limitation in the plots in Figure 5, note they go from -180 to 180 degE.

10. Line 374, "... tend to be aligned...": Well, this seems to be at least partly wishful thinking, I find that it is sometimes true, but sometimes not.

We rephrased the paragraph so it immediately specifies that the tropopause adjustment happens where the wave anomalies are large (see lines 393-395).

11. Line 378, "... cooling and/or warming...": this is not clear to me.

We changed this expression for 'dipole of TP cooling and warming aloft' while rephrasing lines 393-395. We hope that the paragraph involved in points 10 and 11 is more straightforward now.

12. Line 396 and line 401: Figure 5 shows anomalies of $\delta N^2/\delta t$, not anomalies of T!

Thank you for finding this mistake, the terms were corrected accordingly (now in line 407), and the reference to Fig. 5 in the next paragraph was erased. In lines 411-413 now we refer to our method for clarity, since we do filter both T and N^2 fields. Also note that we do not use time derivatives any more in figures 5 and 6, but anomalies (and averaged anomalies), since our earlier interpretation of these quantities was confusing.

13. Line 457, "... a small part...": how do you know that this part is small? Could it be a substantial part?

We erased the term 'small' from this sentence (now in l. 467). We expect the radiative contribution to be small in that equatorial waves are not radiatively driven and their propagation is explained by dry dynamics. We added this explanation in lines 469-471.

14. Line 485, should read: "... would be suited to....".

Thank you for finding this mistake, it's been corrected.

15. Line 525, "... is rather marginal...": "marginal" may not be the right term here. True, it is smaller than in the corresponding figure 3, but it may yet be significant!

We agree. The term 'marginal' was changed for 'very small' (l. 590 and also 298).

References

Dee, D. P., and coauthors,(2011): The ERA-Interim reanalysis: configuration and performance of the data assimilation system, Quarterly Journal of the Royal Meteorological Society, 137, 553-597, doi:10.1002/qj.828.

Poli, P., S. B. Healy, and D. P. Dee (2010): Assimilation of Global Positioning System radio occultation data in the ECMWF ERA-Interim reanalysis, Quarterly Journal of the Royal Meteorological Society, 136, 1972-1990, doi:10.1002/qj.722.

GUIDE TO METEOROLOGICAL INSTRUMENTS AND METHODS OF OBSERVATION (WMO-No. 8) PROVISIONAL 2014 EDITION FOR CIMO-16 APPROVAL. Part I, chapter 13: Measurement of upper wind

http://www.wmo.int/pages/prog/www/IMOP/publications/CIMO-Guide/Provis2014Ed/Provisional2014Ed_P-I_Ch-13.pdf

Response to Referee #2 (Joowan Kim)

We thank Referee #2 (Joowan Kim) for the helpful comments which helped to improve the manuscript significantly. We are particularly grateful for the suggestion about the hydrostatic adjustment mechanism, which clarifies our results in section 3.2. Also, we included a new section 4.3 to discuss how much of the TIL is left without the equatorial wave signal, other mechanisms that could enhance the remaining TIL, and the forcing of the secondary N^2 maximum (as requested in the specific comments). We find that this new subsection puts our results in a better context and makes the paper rounder as a whole.

In the following, we first explain general changes made in the manuscript, and continue with the point-by-point responses to the reviewer's comments. The referee's comments are in blue font, and our replies are in normal font. Every change made in the revised manuscript is highlighted (please find the highlighted version in the Author Response).

General comments:

New subsection 4.3 and Figure 7

Motivated by the specific comments 2 and 3 by Joowan Kim in his review, we added subsection 4.3 to the manuscript in order to discuss how much of the TIL is left without the equatorial wave signal, other mechanisms that could enhance the remaining TIL, and the forcing of the secondary N^2 maximum. Figure 7 compares the time evolution of the equatorial N^2 structure with and without the equatorial wave signal (Thomas Birner asked about this during the SHARP2016 workshop, and we found that making this kind of plot would be the best fit for the purposes of section 4.3).

In Fig. 7 the difference in the TIL region when the equatorial wave signal is subtracted is clear, but the secondary N^2 maximum below the descending westerly QBO phase remains the same, and therefore is not directly modulated by Kelvin waves, as we were suggesting in the discussion manuscript version. Since proven untrue, the paragraphs that discussed the forcing of the secondary N^2 maximum by the filtered Kelvin waves have been erased (now missing from lines 368, 403, 479 and 563), and now we discuss possible forcings in lines 518-527. We still suggest an indirect effect of Kelvin waves (T signal from wave dissipation), but this cannot be captured by our wavenumber-frequency domain filters once the wave dissipates.

New Appendix C

We added a caveat about the filtering of waves with periods of less than 2 days from our daily dataset. Spectral ringing can be an issue with these settings, and could leave a spurious signal in our results (Figure 6), but we checked that the contribution of these periods to the calculated equatorial wave signature of inertia-gravity waves is zero, and therefore doesn't affect our results at all.

Point-by-point responses to Ref#2 (Joowan Kim) comments

Specific comments (minor)

1. The title is too broad for the contents of the manuscript. Authors are mainly focusing on dynamical mechanisms that could enhance TIL in the tropics. Although they demonstrate the mechanisms clearly, the contents in the manuscript are still too limited to cover the whole spectrum of the tropical TIL (e.g., annual cycle, influence of deep convection and radiation, role of shallow Brewer-Dobson circulation). It is strongly recommend for authors to further specify the title of this manuscript.

We changed the title to “The Tropical Tropopause Inversion Layer: Variability and Modulation by Equatorial Waves”, so it's specific to the main results of sections 3 (3D structure and variability) and 4 (effect of equatorial waves).

2. Authors suggest that Kelvin waves cause the enhancement of N2 just below the westerly shear (or zero-wind line) of the QBO. This may be one possible cause, however, the zonal mean temperature anomaly associated with vertical wind shear of the QBO (cf. Fig. 4 in Baldwin et al. 2001) has a strong impact on N2. Several Kelvin of temperature changes in 10 km depth, and this could significantly modulate N2 in the lower stratosphere. In fact, this may have a bigger impact on N2 than Kelvin waves, particularly in zonal mean field. Some analysis and discussion on this effect will be helpful (a simple comparison of tropical mean temperature profiles in westerly and easterly QBO will be good enough).

We prepared a new Figure 7 comparing the N^2 structure with and without the equatorial wave signal, in order to see how much of the TIL and the secondary N^2 maximum are left without it. We found that the secondary N^2 maximum was not affected by the subtraction of equatorial wave anomalies. Therefore, our earlier suggestion that the filtered wave anomalies also contributed to the secondary N^2 maximum was found to be wrong, and any reference to this throughout the paper has been erased (now missing from lines 368, 403, 479 and 563).

We still suggest an indirect effect of Kelvin waves (T signal from wave dissipation), but this cannot be captured by our wavenumber-frequency domain filters once the wave dissipates. This and other possible mechanisms forcing the secondary N^2 maximum are discussed in lines 518-527. We are thankful for the suggestion about the T anomaly associated to wind shear and the reference regarding this, it was added as well into the discussion.

We hope that the new section 4.3 and Figure 7 fulfill the referee's request in this comment, while compensating the erased discussions about the forcing of the secondary N^2 maximum by the filtered equatorial waves.

3. Although influence of deep convection on TIL is beyond the scope of this study, some discussions on tropical convection will still be helpful. For example, the zonal structures in N2 (shown in Fig. 2) are largely related to deep convection in DJF and JJA. In fact, climatology of N2 shows similar structures as in Fig. 2, and this is largely due to tropopause cooling cause by deep convection (deep convection make tropopause colder; e.g., Johnson and Kriete 1982; Gettelman et al. 2002; Paulik and Birner 2012). Only a part of the N2 structure is explained by tropical waves.

In addition, the coherence between N2 and near-tropopause divergence (which is a noble contribution of this paper) is consistent with the hydrostatic adjustment mechanism, which is proposed by Holloway and Neelin (2007) to explain cold-top (tropopause) over deep convection. Those discussion could be helpful for readers.

We added a discussion about other TIL forcing mechanisms in the new section 4.3. Figure 7b shows the remaining, much weaker TIL without the equatorial wave signal. We also include the hydrostatic adjustment mechanism when convection is not wave-coupled and radiative forcing as possible TIL enhancers in this discussion (lines 496-502).

Also, we are very grateful for the suggestion about the hydrostatic adjustment mechanism, regarding the relation between stronger TIL and near-tropopause divergent flow. We added a paragraph in section 3.2 (lines 300-307) discussing this, which improves the explanation about the sTIL relationship with divergence and makes it clearer.

Technical suggestions

Line 35: Satellite GPS => Global Positioning System (GPS) (In many place, satellite GPS => GPS)

We only keep the word 'satellite' the first time we refer to GPS-RO in case any reader is not familiar with this dataset, and we follow the suggestion the rest of the times GPS is referred to.

Line 105: tropopause height (TPz) using the WMO lapse-rate tropopause criterion...

Corrected.

Line 169: latitude (y) and time (t). The maximum distance allowed from the grid point in each dimension is 5°longitude, 10°longitude, and 12 hours, respectively.

Corrected.

Line 214: 3.1 ?

True, there was a title missing! We titled section 3 “Structure and Variability of the Tropical TIL”, and subsection 3.1 “Vertical and Horizontal Structures”.

Line 234: 2011=>2010?

Thank you for finding this mistake, it was corrected (now in lines 235 and 241).

Line 375: highest amplitude => maximum amplitude

Corrected.

Line 379: very high => very large

Corrected.

Line 393: high amplitude => large amplitude

Corrected.

Line 476: higher that within => larger than that in

Corrected.

Fig 5: why do you show N2 tendency (dN2/dt) instead of N2?
(also in Fig 6: dT/dt instead of T)?

We now show these parameters as anomalies (or averaged anomalies) in both figures 5 and 6. The way we interpreted these quantities was confusing in the earlier manuscript, we hope it is more straightforward now.

Response to Referee #3

We thank Referee #3 for the helpful comments which helped to improve the manuscript significantly. We are particularly grateful for the suggestion about the hydrostatic adjustment mechanism, which clarifies our results in section 3.2.

In the following, we first explain general changes made in the manuscript, and continue with the point-by-point responses to the reviewer's comments. The referee's comments are in blue font, and our replies are in normal font. Every change made in the revised manuscript is highlighted (please find the highlighted version in the Author Response).

General comments:

New subsection 4.3 and Figure 7

Motivated by the specific comments 2 and 3 by Joowan Kim in his review, we added subsection 4.3 to the manuscript in order to discuss how much of the TIL is left without the equatorial wave signal, other mechanisms that could enhance the remaining TIL, and the forcing of the secondary N^2 maximum. Figure 7 compares the time evolution of the equatorial N^2 structure with and without the equatorial wave signal (Thomas Birner asked about this during the SHARP2016 workshop, and we found that making this kind of plot would be the best fit for the purposes of section 4.3).

In Fig. 7 the difference in the TIL region when the equatorial wave signal is subtracted is clear, but the secondary N^2 maximum below the descending westerly QBO phase remains the same, and therefore is not directly modulated by Kelvin waves, as we were suggesting in the discussion manuscript version. Since proven untrue, the paragraphs that discussed the forcing of the secondary N^2 maximum by the filtered Kelvin waves have been erased (now missing from lines 368, 403, 479 and 563), and now we discuss possible forcings in lines 518-527. We still suggest an indirect effect of Kelvin waves (T signal from wave dissipation), but this cannot be captured by our wavenumber-frequency domain filters once the wave dissipates.

New Appendix C

We added a caveat about the filtering of waves with periods of less than 2 days from our daily dataset. Spectral ringing can be an issue with these settings, and could leave a spurious signal in our results (Figure 6), but we checked that the contribution of these periods to the calculated equatorial wave signature of inertia-gravity waves is zero, and therefore doesn't affect our results at all.

Point-by-point responses to Ref#3 comments

Major Comments:
1) divergence-TIL relationship:
The relation of TIL strength to tropopause-level divergence is new and interesting. But what I find puzzling is that convergence apparently does not lead to a reduction in TIL strength (Fig. 3). For DJF TIL strength is independent of the strength of convergence (Div < 0), for JJA it even increases slightly for strong convergence. This seems to contradict the mechanism put forward in section 3.2 (vertical gradient of vertical velocity forcing N^2) and should be discussed/interpreted somewhere in the paper.

Another question I have related to the divergence-TIL relation is: what is the impact of deep convective outflow? Strong tropopause-level divergence would be expected from organized deep convection. Deep convection is known to be associated with the "cold top" (e.g. Holloway & Neelin, 2007; or Paulik & Birner, 2012 who quantified this using COSMIC data) – a strong tropopause-level cold anomaly aloft mid-to-upper tropospheric heating, which should be associated with enhanced TIL. This signal would primarily show up for strong meso- to large-scale divergence. I wonder whether this in part explains the relationship shown in Fig. 3? For large-scale convergence the TIL may locally still be enhanced due to smaller scale dynamics (e.g. gravity waves) and the tropopause-following coordinate.

We are grateful for the suggestion about the hydrostatic adjustment mechanism, regarding the relation between stronger TIL and near-tropopause divergent flow from convection. We added a paragraph in section 3.2 (lines 300-307) discussing this, which improves the explanation about the sTIL relationship with divergence and makes it clearer. We link the vertical wind convergence term to convection as well, since it only has an effect on the TIL with divergent flow (convective outflow). We now suggest that vertical wind convergence is one mechanism enhancing the TIL at all latitudes, but caused by different processes: convection in the tropics and baroclinic waves in the extratropics. This interpretation is added in lines 317-322.

2) wave-modulation of tropopause
I found the portrayal of the wave-modulation of the tropopause and TIL somewhat confusing. Section 4 is titled "Dynamical Forcing by Equatorial Waves", but what is primarily shown is the quasi-reversible transient modulation. Any wave with a vertical temperature signature will have layers of positive temperature gradient (enhanced stratification) and layers of negative temperature gradient (reduced stratification). By definition, if the wave propagates through the tropopause, the tropopause algorithm will place the local tropopause near the wave-induced temperature minimum, which, again by definition, puts the layer of enhanced stratification (TIL) just above the local tropopause. From that perspective, the TIL enhancement is just a quantification of the wave itself, so cannot be considered a response to the wave (as would be implied by "forcing"). It also doesn't allow the TIL to be considered part of the basic state structure for wave propagation (see authors' motivation in 2nd paragraph of abstract and introduction).

I would urge the authors to be more careful with the wording and interpretations in section 4: what is quantified is the wave-modulation of the tropopause (incl. its TIL structure), not the wave-forcing. It is not clear how much of the analyzed signals are reversible vs. irreversible – possibly, a life-cycle analysis of certain wave types might reveal how much of the wave-modulation is left over once the wave has passed through the region.

We agree that the use of the term 'forcing' might not be the most correct, it's a good point that it shall rather be considered as an instantaneous modulation. We substituted the term 'forcing' for 'modulation' throughout the paper, also for 'signal' or 'signature' where it was most convenient. We discuss the possibility of further (more permanent) effects of the waves once they leave the tropopause (or dissipate), which could enhance the TIL as well, in lines 513-517.

Regarding the wave signature as a mere quantification of the wave itself, it shall not be viewed as an artifact of the tropopause-coordinate following. Although transient and instantaneous, there are motions associated to the wave signal that locally lift/cool/modulate the tropopause, and also warm the air aloft. Another characteristic of the waves is that they amplify next to and above the tropopause (Fig. 5), and also increase their vertical tilt (Fig. 5a, visible for Kelvin waves), which increases the wave signal in the TIL region, and also increases the area of positive N^2 anomaly above the tropopause. This is a response of the wave to the elevated N^2 values in the lowermost stratosphere, in agreement with linear theory, which in turn enhances the TIL further, working as a TIL-enhancing feedback. We discuss this in lines 480-489, while specifying that more research needs to be done to ascertain such feedback as a robust feature of the tropopause region.

We prefer not to discuss whether the TIL shall be considered part of the basic state structure for wave propagation in our manuscript since it's beyond the scope of our study, and our current results are not enough to fully support (or deny) this. Nevertheless, our results suggest that there is a response of the wave to the higher N^2 values in the lowermost stratosphere (Fig. 5a), which is predicted by theory. But again more research needs to be done in this respect in order to make a robust statement.

3) discussion of applicability to extratropics:
I suggest to either expand Section 5 or remove it – it’s not much of a discussion at this point, other than to simply note that there are waves in the extratropics and that a similar analysis could be performed there. The way it stands it would suffice to simply mention this in section 6. If the authors feel it’s important to include this section then it should discuss in what way the findings might carry over to the extratropics (or not), given the very different dynamical constraints and physically distinct waves. But again, I don’t really see the point of including such a discussion – it seems to primarily distract from the main points of the paper.

Since the submission of the manuscript, there have been developments regarding the application of our method in the extratropics: the method is successful in quantifying the modulation and enhancement of the TIL in the extratropics by extratropical waves, and we are preparing an upcoming paper about this.

We would prefer to keep this section (with some rephrasing in lines 544-548), since it is important to state the usefulness of our method outside the equator. Also note that we do discuss about what is to be expected in the extratropics: see the discussion about baroclinic Rossby waves in lines 531-538 (which are expected to have a bigger signature than Kelvin or any equatorial wave). The role of inertia-gravity waves in enhancing the extratropical TIL is predicted from the modelling study by Kunkel et al. (2014), but is still awaiting confirmation from observations.

Minor comments:

Abstract: the first two paragraphs are very general/generic and can probably be condensed into one shorter paragraph.

We merged both paragraphs into one, slightly reducing its length where possible.

line 16: do you mean that you approximate the meteorological situation by the 100 hPa divergence field? The divergence field certainly doesn't completely determine the meteorological situation.

We agree in that we do not show a full meteorological description of the tropical tropopause, but only TIL-relevant parameters. We erased the word 'meteorological' to make the sentence simpler.

line 18: "new feature": I agree that this is quantified better here, but the QBO–static stability relation was already described in Grise et al. (2010), so by itself is not new

We agree that Grise et al. (2010) shows a correlation of enhanced N^2 in the layer 1-3 above the tropopause and throughout the lower-mid stratosphere following the easterly phase of the QBO. However, in that paper there is no reference that this correlation creates a second N^2 maximum that is close to TIL strength. We feel that it is justified to call it a new feature.

line 36: I believe Randel et al. (2007) were the first to demonstrate this from GPS

In the paper by Randel et al. (2007) the term 'global' is used in a very nuanced way: they show the "global structure of the *extratropical* TIL". The tropics and the equator are not investigated in this paper. Grise et al. (2010) is the first publication to explore the TIL globally in the literal sense: covering the extratropics and tropics, therefore we would like to keep the reference as is.

line 52: Randel et al. (2007) were the first to suggest this mechanism

We agree, we added this reference in the text.

line 70/71: Grise et al. show a lag-regression of N^2 to QBO index, which includes the entire lower-to-mid stratosphere

We agree and we refer to this later in section 3.1.1, but we feel that including this into a TIL-relevant introduction is unnecessary.

line 91: 100 m is the resolution at which the data is provided, which is not the same as the effective physical resolution – please include corresponding remark (see referenced papers on GPS data for details)

We added the corresponding remark in lines 90-91.

line 101: it's -> it is (and similarly at other places)

We corrected this throughout the paper.

line 110: I suggest parentheses around (g/theta)

We added parentheses for both terms in the equation.

line 125: remove “empty”

Corrected.

line 176: remove “a” before “6.5%”

Corrected.

line 200 (and at other places): usually the n=0 mode is referred to as mixed-Rossby-gravity (MRG) wave (or Yanai wave) – please clarify

We added a clarification in lines 206-207: we don't use these terms for simplicity, since there's already a considerable array of wave types that we filter and constantly refer to throughout the paper.

line 234 (and other places): referring to the QBO-associated static stability maximum as secondary TIL could be confusing, as it’s not always located near the tropopause – I suggest to distinguish those; another potential issue is that Grise et al. already referred to a secondary TIL at the poleward flanks of the inner tropics, which is different from what is referred to as secondary TIL here

We added a specification in lines 239-240 that this secondary maximum shall not be considered a second TIL. Note that throughout the paper we differentiate between TIL and this secondary maximum (see line 251, 335, 363), and that this secondary N^2 maximum is never referred to as a second TIL, only that it leads to a double-TIL-like structure in static stability (because it looks like it in the stability profile, but the second maximum is far away from the tropopause, and strictly speaking there is no temperature inversion given the background temperature lapse-rate in the stratosphere).

In the paper by Grise et al. (2010) there is reference to two distinct features in static stability (in the layers 0-1 and 1-3 km above the tropopause), not to a secondary TIL.

line 285 (and other places): I suggest “analogous” instead of “similar” for the comparison between vorticity-TIL and divergence-TIL relations (vorticity and divergence are distinct meteorological fields, so “similar” may be confusing to some readers)

Thank you for this suggestion, we proceeded with this change throughout the paper.

line 302: “absence of Coriolis force” – I don’t understand this comment, isn’t this just referring to the continuity Eq., which doesn’t depend on the Coriolis force?

We now see that this sentence was misleading in the way it was written: we wanted to imply that in the tropics the vertical convergence term is not related to relative vorticity. We erased that part of the sentence for simplicity (line 317 now), since parts of section 3.2 have been rephrased and the separation of the processes driving vertical convergence in the tropics/extratropics are clear now.

line 364 / Figs. 5, 6: why did you decide to show the time-derivatives of T and N^2 (as opposed to just T and N^2)? This came as a surprise to me, so I’d suggest to include a brief statement motivating this choice.

We now show these parameters as anomalies (or averaged anomalies) in both figures 5 and 6. The way we interpreted these quantities was confusing in the earlier manuscript, we hope it is more straightforward now.

Manuscript prepared for Atmos. Chem. Phys.
with version 2015/04/24 7.83 Copernicus papers of the LaTeX class copernicus.cls.
Date: 2 June 2016

The Tropical Tropopause Inversion Layer: Variability and Modulation by Equatorial Waves

Robin Pilch Kedzierski[1], Katja Matthes[1,2], and Karl Bumke[1]

[1]Marine Meteorology Department, GEOMAR Helmholtz Centre for Ocean Research Kiel, Kiel, Germany.

[2]Faculty of Mathematics and Natural Sciences, Christian-Albrechts-Universität zu Kiel, Kiel, Germany.

Correspondence to: Robin Pilch Kedzierski (rpilch@geomar.de)

Abstract.

The Tropical Tropopause Layer (TTL) acts as a 'transition' layer between the troposphere and the stratosphere over several kilometers, where air has both tropospheric and stratospheric properties. Within this region, a fine-scale feature is located: the Tropopause Inversion Layer (TIL), which consists of a sharp temperature inversion at the tropopause and the corresponding high static stability values right above, which theoretically affect the dispersion relations of atmospheric waves like Rossby or Inertia-Gravity waves and hamper stratosphere-troposphere exchange (STE). Therefore, the TIL receives increasing attention from the scientific community, mainly in the extratropics so far. Our goal is to give a detailed picture of the properties, variability and forcings of the tropical TIL, with special emphasis on small-scale equatorial waves and the QBO.

We use high-resolution temperature profiles from the COSMIC satellite mission, i.e. ∼2000 measurements per day globally, between 2007 and 2013, to derive TIL properties and to study the fine-scale structures of static stability in the tropics. The situation at near tropopause level is described by the 100hPa divergence fields, and the vertical structure of the QBO is provided by the equatorial winds at all levels, both from the ERA-Interim reanalysis.

We describe a new feature of the equatorial static stability profile: a secondary stability maximum below the zero wind line within the easterly QBO wind regime at about 20-25km altitude, which is forced by the descending westerly QBO phase and gives a double-TIL-like structure. In the lowermost stratosphere, the TIL is stronger with westerly winds. We provide the first evidence of a relationship between the tropical TIL strength and near-tropopause divergence, with stronger (weaker) TIL with near-tropopause divergent (convergent) flow, a relationship analogous to that of TIL strength with relative vorticity in the extratropics.

To elucidate possible enhancing mechanisms of the tropical TIL, we quantify the signature of the different equatorial waves on the vertical structure of static stability in the tropics. All waves show maximum cooling at the thermal tropopause, a warming effect above, and a net TIL enhancement close to the tropopause. The main drivers are Kelvin, inertia-gravity and Rossby waves. We suggest

that a similar wave modulation will exist at mid and polar latitudes from the extratropical wave modes.

1 Introduction

The Tropopause Inversion Layer (TIL) is a narrow region characterized by temperature inversion and enhanced static stability located right above the tropopause. This fine-scale feature was discovered by tropopause-based averaging of high-resolution radiosonde measurements by Birner et al. (2002) and Birner (2006). Satellite Global Positioning System radio occultation observations (GPS-RO) show that the TIL is present globally (Grise et al., 2010).

Static stability is a parameter used in a number of wave theory approximations, thus affecting the dispersion relations of atmospheric waves like Rossby or Inertia-Gravity waves (Birner, 2006; Grise et al., 2010). Also, static stability suppresses vertical motion and correlates with sharper trace gas gradients, inhibiting the cross-tropopause exchange of chemical compounds (Hegglin et al., 2009; Kunz et al., 2009; Schmidt et al., 2010). For these reasons, the TIL attracts increasing interest from the scientific community.

There is a considerable body of research about the TIL in the extratropics, establishing the TIL as an important feature of the extratropical upper-troposphere and lower-stratosphere (Gettelman et al., 2011). In the tropics, the transition between the troposphere and the stratosphere is considered to happen over several kilometers, dynamically and chemically (Fueglistaler et al., 2009; Gettelman and Birner, 2007), but less is known about the tropical TIL, as the following review will show.

In the extratropics, climatological studies have shown that the TIL reaches maximum strength during polar summer (Birner, 2006; Randel et al., 2007; Randel and Wu, 2010; Grise et al., 2010), whereas the TIL within anticyclones in mid-latitude winter is of the same strength or even higher from a synoptic-scale point of view (Pilch Kedzierski et al., 2015). Several mechanisms for extratropical TIL formation/maintenance have been studied: water vapor radiative cooling below the tropopause (Randel et al., 2007; Hegglin et al., 2009; Kunz et al., 2009; Randel and Wu, 2010), dynamical heating above the tropopause from the downwelling branch of the stratospheric residual circulation (Birner, 2010), tropopause lifting and sharpening by baroclinic waves and their embedded cyclones-anticyclones (Wirth, 2003, 2004; Wirth and Szabo, 2007; Son and Polvani, 2007; Randel et al., 2007; Randel and Wu, 2010; Erler and Wirth, 2011), and the presence of small-scale gravity waves (Kunkel et al., 2014). A high-resolution model study by Miyazaki et al. (2010a, b) suggests that radiative effects dominate TIL enhancement in polar summer whereas dynamics are the main drivers in the remaining latitudes and seasons.

On the other hand, very little research has focused on the tropical TIL. Bell and Geller (2008) showed the TIL from one tropical radiosonde station, and Wang et al. (2013) reported a slight weakening of the tropical TIL between 2001-2011. Grise et al. (2010) included the horizontal and vertical variability of the tropical TIL in their global study about near-tropopause static stability, which is so far the most detailed description of the TIL in the tropics. They found the strongest TIL centered at the equator in the layer 0-1km above the tropopause, peaking during NH winter. This agrees well with the seasonality and location of tropopause sharpness as described later by Son et al. (2011) and Kim and Son (2012). The horizontal structures in seasonal mean TIL in the tropics are reminiscent of the equatorial stationary wave response associated with climatological deep convection (Grise et al., 2010; Kim and Son, 2012). Grise et al. (2010) also noted that static stability is enhanced in the layer 1-3km above the tropopause during the easterly phase of the quasi-biennial oscillation (QBO).

Equatorial waves influence the intraseasonal and short-term variability of the temperature structure near the tropical tropopause (Fueglistaler et al., 2009). Kelvin waves and the Madden-Julian oscillation (MJO) (Madden and Julian, 1994) were reported as the dominant modes of temperature variability at the tropopause region (Kim and Son, 2012). Equatorial waves cool the tropopause region (Grise and Thompson, 2013), and also produce a warming effect above it (Kim and Son, 2012). This wave effect forms a dipole that can sharpen the gradients that lead to TIL enhancement, but no study has quantified this effect so far.

Our study aims to describe the tropical TIL, its variability and forcings in detail, in order to increase the knowledge about its properties and highlight this sharp and fine-scale feature within the tropical transition layer between the troposphere and the stratosphere. Section 2 will show the datasets and methods used in our analyses. Section 3 will describe the vertical and horizontal structure and day-to-day variability of the TIL, its relationship with near-tropopause divergence, and the influence of the QBO on the vertical structure of static stability and TIL strength in particular. In section 4 we quantify the signature of the different equatorial waves and their effect on the mean temperature and static stability profiles in tropopause-based coordinates. Section 5 will discuss the applicability of our results with equatorial wave modulation to the extratropical TIL, given the different wave spectrum in the extratropics, and section 6 sums up the results.

2 Data and Methods

2.1 Datasets

We analyze temperature profiles from GPS radio occultation (GPS-RO) measurements. These are provided with a high vertical resolution of 100m (although the effective physical resolution of the retrievals is even better), from the surface up to 40km altitude, comparable to high-resolution radiosonde data. The advantage of GPS-RO is based on its global coverage, high sampling density of ∼2000 profiles/day, and weather-independence. We mainly use data from the COSMIC satellite mission (Anthes et al., 2008) for the years 2007-2013. For Figure 1 only, we added two earlier GPS-RO satellite missions: CHAMP (Wickert et al., 2001) and GRACE (Beyerle et al., 2005), which provide less observations (around 200 profiles/day together) for 2002-2007.

The situation at near-tropopause level is retrieved from the ERA-Interim reanalysis (Dee et al., 2011). We make use of divergence and geopotential height fields at 100hPa on a 2.5°×2.5° longitude-latitude grid and 6-hourly time resolution, and also daily-mean vertical profiles of the zonal wind at the equator, for the time period 2007-2013. We choose the 100hPa level because it is the standard pressure level from ERA-Interim that is closest to the climatological tropopause in the tropics (96-100hPa in summer, 86-88hPa in winter, Kim and Son (2012)). Tropical winds near the tropopause in ERA-Interim differ from observations slightly more than in the extratropics, but still are of good quality (Poli et al., 2010; Dee et al., 2011).

2.2 TIL Strength Calculation

We define the tropopause height (TP_z) using the WMO lapse-rate tropopause criterion (WMO, 1957). Given the strong negative lapse-rate found above the tropopause near the equator, the lapse-rate tropopause nearly coincides with the cold-point tropopause most of the time. This is in agreement with earlier studies, which did not find substantial differences in their results applying different tropopause definitions (Grise et al., 2010; Wang et al., 2013). From the GPS-RO temperature profiles, vertical profiles of static stability are calculated as the Brunt-Väisälä frequency squared (N^2 [s^{-2}]):

$$N^2 = (g/\Theta) \cdot (\partial\Theta/\partial z)$$

where g is the gravitational acceleration, and Θ the potential temperature. Profiles with unphysical temperatures or N^2 values (temperature <-150°C, >150°C or N^2 >$100\times10^{-4}s^{-2}$) and those where the tropopause cannot be found have been excluded. TIL strength (sTIL) is calculated as the maximum static stability value (N^2_{max}) above the tropopause level. This sTIL measure is commonly used (Birner et al., 2006; Wirth and Szabo, 2007; Erler and Wirth, 2011; Pilch Kedzierski et al., 2015), because it makes sTIL independent of its distance from the tropopause and N^2 is a physically relevant quantity. Our algorithm searches for N^2_{max} in the first 3km above TP_z, but most often finds it in the first kilometer.

2.3 Mapping of TIL Snapshots

The procedure to derive daily TIL snapshots in this study is similar to the method by Pilch Kedzierski et al. (2015), but with a longitude-latitude projection.

The daily TIL snapshots were estimated at a 5° longitude-latitude grid between 30°S-30°N. For each grid point we calculate the mean N^2_{max} from all GPS-RO profiles within +-12.5° longitude-latitude to account for the lower GPS-RO observation density in the tropics compared to the extratropics (Son et al., 2011). This setting avoids gaps appearing in the maps, and smooths out undesired small-scale features that cannot be captured with the current GPS-RO sampling.

We also produce similar maps of 100hPa divergence. For a fair comparison with the TIL snapshots, we equal the spatial scale and follow the same method, but instead of averaging N^2_{max} values, we use the collocated divergence of each GPS-RO profile: the value from the nearest ERA-Interim grid point and 6h time period to each observation. Examples of TIL snapshots can be found in Figure 2 (section 3.1.2). If plotted at full horizontal resolution, divergence would show small-scale features superimposed over the synoptic-to-large scale structures in Fig. 2, making the comparison with N^2_{max} more difficult.

2.4 Wavenumber-Frequency Domain Filtering

Our purpose is to extract the temperature and N^2 signature of the different equatorial wave types on the zonal mean vertical profiles. For this, we follow Wheeler and Kiladis (1999), that studied equatorial wave signatures on the outgoing longwave radiation (OLR) spectrum observed from satellites by wavenumber-frequency domain filtering. Wheeler and Kiladis (1999) give an in-depth description of the theoretical and mathematical background of the filtering methods.

Theoretically, the equatorial wave modes are the zonally and vertically propagating, equatorially trapped solutions of the 'shallow water' equations (Matsuno, 1966; Lindzen, 1967) characterized by four parameters: meridional mode number (*n*), frequency (*v*), zonal planetary wavenumber (*s*) and equivalent depth (*h*). Each wave type (Kelvin, Rossby, the different modes of Inertia-Gravity waves) has a unique dispersion curve in the wavenumber-frequency domain, given its mode *n* and equivalent depth *h*.

Wheeler and Kiladis (1999) found that the equatorial OLR power had spectral signatures that were significantly above the background. The signature's regions in the wavenumber-frequency domain match with the dispersion curves of the different equatorial wave types. Also, they found signatures outside of the theoretical wave dispersion curves that have characteristics of the Madden-Julian oscillation (MJO) (Madden and Julian, 1994).

Our method is similar to that of Wheeler and Kiladis (1999), but analyzes temperature and N^2 at all levels between 10-35km altitude instead of OLR. For filtering, the data must be periodic in longitude and time and cover all longitudes of the equatorial latitude band. Therefore, the COSMIC GPS-RO profiles (Anthes et al., 2008) need to be put on a regular longitude grid on a daily basis. We explain how this is done in the follwing section (2.4.1). More details about our proceeding with the filter, and the differences from Wheeler and Kiladis (1999) can be found in section 2.4.2. Note that this method is only used in Figs. 5 and 6 (section 4).

2.4.1 Gridding of GPS-RO profiles

The COSMIC GPS-RO temperature profiles between 10°S-10°N are gridded daily on a regular longitude grid with a 10° separation. At each grid point, the profiles of that day within 10°S-10°N and

+-5° longitude are selected to calculate a tropopause-based weighted average temperature profile and the corresponding N^2 vertical profile:

$$T_{grid}(\lambda, Z_{TP}, t) = \sum_i w_i T_i(\lambda, Z_{TP}, t) / \sum_i w_i$$

$$N^2_{grid}(\lambda, Z_{TP}, t) = \sum_i w_i N^2_i(\lambda, Z_{TP}, t) / \sum_i w_i$$

where λ is longitude, Z_{TP} is the height relative to the tropopause and t is time. The weight w_i is an exponentially-folding function that depends on the distance of the GPS-RO profile from the grid center, taking longitude, latitude and time (distance from 12UTC):

$w_i = exp(-[(D_x/5)^2 + (D_y/10)^2 + (D_t/12)^2])$, where D are the distances in °longitude (x subscript), °latitude (y) and hours (t). The maximum distance allowed from the grid point in each dimension is: 5° longitude, 10° latitude, and 12 hours from 12UTC, respectively.

The gridded tropopause height (λ,t) is calculated with the same weighting of all profiles' tropopauses. The gridded temperature and N^2 profiles are shifted, as the last step, from the tropopause-based vertical scale onto a ground-based vertical scale from 10km to 35km altitude, obtaining a longitude-height array for each day for 2007-2013.

Most often 2-3 profiles are selected for averaging at a grid point with these settings, although one GPS-RO profile is sufficient to estimate a grid point. However, in 6.5% of the cases the algorithm does not find any profile. To fill in the gaps, the longitude range to select the profiles is incremented to +-10° instead of +-5°, which still leaves a 0.8% of empty grid-points. For this minority, profiles are selected within +-1day and +-15° longitude. In all cases the weighting function remains the same. These exceptions are for a very small portion of the gridded data, and therefore do not affect the retrieved wave signatures after filtering.

Our method is essentially an update from Randel and Wu (2005). It is adapted for the higher number of GPS-RO retrievals of the COSMIC mission compared to its predecessors CHAMP and GRACE: Randel and Wu (2005) used a 30° longitude grid and selected profiles for +-2days, while we use 10° spacing and profiles of the same day. This leads to increased zonal resolution, as well as a minimized temporal smoothing. Another difference is that we do the averaging in tropopause-based coordinates to avoid smoothing the TIL, and also use latitude differences in the weighting function. Compared to earlier studies that filtered equatorial waves using GPS-RO data (Randel and Wu, 2005; Kim and Son, 2012), our daily fields with barely any running mean allow the analysis of waves with higher frequencies and wavenumbers (i.e. a wide part of the inertia-gravity wave spectrum) that otherwise are smoothed out and not accounted for.

2.4.2 Filter Settings

With the longitude-height-time array of gridded temperature and N^2 profiles obtained according to section 2.4.1, we proceed with the filtering in the wavenumber-frequency domain as follows. For each vertical level (from 10km to 35km height with 0.1km vertical spacing), a longitude-time array is retrieved, detrended and tapered in time. Then, a space-time bandpass filter is applied using a two-dimensional Fast Fourier Transform. This is done using the freely available 'kf-filter' NCL function (Schreck, 2009).

The bandpass filter bounds in the wavenumber-frequency domain are defined for the following wave types: Kelvin waves, Rossby waves, and all modes of Inertia-Gravity waves: n = (0,1,2). We separate westward-propagating (negative wavenumber s) Inertia-Gravity waves (WIG_n), the eastward-propagating ones (positive s, EIG_n), and the zonal wavenumber zero ($_{s=0}IG_n$) in the analysis. We do not use the terms Mixed-Rossby-Gravity wave (MRG) or Yanai wave for the n = 0 modes throughout the manuscript for simplicity. Including the MJO band (which does not belong to any theoretical dispersion curve), we end up with 12 different bandpass filters that are applied to the longitude-time array of gridded temperature and N^2, at each vertical level separately. The exact filter bounds are listed in Table 1. They are similar to the ones used by Wheeler and Kiladis (1999) and take into account the faster and not convectively coupled Kelvin waves found by Kim and Son (2012) in the tropopause temperature variability spectrum. We also allow faster WIG_0 and Rossby waves in the corresponding filters. Note that the filter bounds defined in Table 1 never overlap in the wavenumber-frequency domain. After filtering, we obtain a daily longitude-height section with the 12 waves' temperature and N^2 signatures. We stress that the temperature and N^2 fields are filtered independently at each vertical level.

3 Structure and Variability of the Tropical TIL

3.1 Vertical and Horizontal Structures

3.1.1 Temporal variability of the vertical N^2 profile

We first focus on the variation of the equatorial N^2 profiles over time. Figure 1 shows the daily evolution of the equatorial (5°S-5°N) zonal mean N^2 profile between 2002-2013, with zonal wind contours superimposed (black westerlies, and dashed easterlies), and a grey tropopause line. The years 2002-2006 appear noisier because the number of observations from the CHAMP (Wickert et al., 2001) and GRACE (Beyerle et al., 2005) satellite missions is about 10 times less than the amount of profiles from COSMIC (Anthes et al., 2008) used between 2007-2013. Therefore local anomalies have a bigger impact on the zonal mean vertical profile during 2002-2006.

The tropopause height in Fig. 1 has a seasonal cycle with a generally higher (lower) tropopause and higher (lower) values of N^2 right above it during the NH winter (summer) months, in agreement with the seasonal cycle of the tropopause (Yulaeva et al., 1994) and the tropical TIL climatological seasonal cycle described by Grise et al. (2010).

The daily evolution of N^2 also shows a secondary maximum below the zero wind line (bold black), at the easterly side of the descending westerly QBO phase, between 20-25km height. The zero wind line (of the descending westerly QBO phase) usually crosses the ∼20km level in summer, while crossing the ∼25km level in the earlier winter. This happens in 2002, 2004, 2006, 2008 and 2013, with the exception of 2010 when the zero wind line crosses ∼25km in summer. The enhanced N^2 is present under the zero wind line all the way from 35km altitude, but it is most evident in winter and spring (∼25km altitude and below). In winter and spring the secondary maximum of N^2 (red, about $8\times10^{-4}s^{-2}$) is close to the TIL strength (brown, about $9\times10^{-4}s^{-2}$ in the first kilometer above the tropopause), forming a double-TIL-like structure in static stability. However, this secondary maximum in N^2 shall not be viewed as a second TIL since it is quite far away from the tropopause. In the case of 2010, when the secondary maximum appears in summer it is much weaker, probably due to the fact that N^2 is generally weaker throughout the whole lower stratosphere in summer (Fig. 1). We also note that during the descending easterly QBO phase N^2 is enhanced above the zero wind line, again within the easterly wind regime. This time, the enhanced N^2 is much weaker than in the descending westerly QBO phase case, and only discernible in the lowermost stratosphere.

Grise et al. (2010) found a significant correlation of enhanced N^2 in the layer 1-3km above the TP when easterlies were present in the lowermost stratosphere, while no clear correlation was found in the 0-1km layer above the TP. From Fig. 1 we deduce that this correlation of the 1-3km layer originates in the secondary N^2 maximum found below the zero wind line of the descending westerly QBO (or above the zero line of the descending easterly QBO to a lesser degree, within the easterly QBO wind regime in any case). The QBO influence on the TIL, strictly the absolute N^2_{max} that is found in the first kilometer above the TP, is hard to discern in Fig. 1. We investigate this in more detail in the subsection 3.3.

3.1.2 Horizontal structure of TIL strength

Figure 2 shows daily snapshots of TIL strength (sTIL, N^2_{max}) and collocated divergence (see section 2.4.1) between 30°S-30°N, together with 100hPa geopotential height contours, for four different days: two winter cases (left) and two summer cases (right), as examples representative of the variability in strength and zonal structures of the tropical TIL between 2007 and 2013.

The first remarkable aspect of the tropical TIL is that the magnitude of N^2_{max} is much higher than in the extratropics. Values near the equator vary between 9-15 $\times10^{-4}s^{-2}$ and reach the $20\times10^{-4}s^{-2}$ mark sometimes, compared to a sTIL of 8-10$\times10^{-4}s^{-2}$ generally found in polar summer or within ridges in mid-latitude winter (Pilch Kedzierski et al., 2015). This can be attributed to the background temperature gradient in the lower stratosphere in the tropics, with a strong negative lapse-rate and a higher background lower-stratospheric N^2.

When a dipole of tropopause cooling and warming aloft (needed for TIL formation) is added to this background profile, the potential temperature gradient just above the tropopause increases dramatically, giving the enormous N^2_{max} values observed in Fig. 2.

The peak containing N^2_{max} is very narrow and not always found at the exact same distance from the tropopause. Thus, when a zonal mean N^2 profile is computed, the high N^2_{max} values get slightly smoothed out (Pilch Kedzierski et al., 2015). This is why the N^2 values in the first kilometer above the tropopause in Fig. 1 are lower than in Fig. 2.

As observed by Grise et al. (2010), in Fig. 2 we find that the strongest TIL is almost always centered at the equator, pointing towards equatorially trapped wave modes as TIL enhancers (which we analyze in section 4). When the sTIL zonal structure is compared to 100hPa divergence and geopotential height, it can be observed that higher N^2_{max} is in general near regions of divergent flow (blue in Fig. 2) and a higher 100hPa surface. This high-low behavior with stronger-weaker TIL highly resembles the cyclone-anticyclone relationship with sTIL found in the extratropics (Randel et al., 2007; Randel and Wu, 2010; Pilch Kedzierski et al., 2015).

So far, Figs. 1 and 2 confirm the vertical/horizontal structures of the TIL and its seasonality from earlier studies Grise et al. (2010); Kim and Son (2012), while reporting new features: the TIL relation with near-tropopause divergence (which we analyze next in section 3.2) and a secondary N^2 maximum above the TIL region driven by the QBO, whose influence on the TIL is analyzed in section 3.3.

3.2 Relationship with Divergence

In this subsection, we have a closer look at the relationship of the zonal structure of the tropical sTIL with its collocated divergence as shown in Fig. 2. For this, we bin sTIL and tropopause height depending on the divergence value collocated with each GPS-RO observation, and make a mean within each divergence bin, as previous studies did with relative vorticity in the extratropics (Randel et al., 2007; Randel and Wu, 2010; Pilch Kedzierski et al., 2015). The resulting divergence versus sTIL diagrams are shown in Figure 3. In both summer and winter (Figs. 3 a, b) sTIL increases with divergence: from 11-12$\times 10^{-4} s^{-2}$ found with convergent flow (negative values) or near-zero divergence, increasing steadily up to almost $15\times 10^{-4} s^{-2}$ with increasingly divergent flow. The sTIL relation with divergence shown in the diagrams from Figs. 3 a and b is analogous to that of relative vorticity versus sTIL in the extratropics from earlier studies (Randel et al., 2007; Randel and Wu, 2010; Pilch Kedzierski et al., 2015). We also note that the N^2_{max} in winter is always slightly higher than in summer for any divergence value, in agreement with the seasonality with stronger TIL in winter from Fig.1 and the climatology by Grise et al. (2010). There is no clear link between a higher tropopause and a stronger TIL. The variation of tropopause height with divergence is very small (see Appendix A, figure A1).

The relation of stronger TIL with divergent flow in Fig. 3 is consistent with the hydrostatic adjustment mechanism over deep convection described by Holloway and Neelin (2007), which results in a colder tropopause and an increased temperature gradient aloft. Paulik and Birner (2012) showed that this negative temperature signal near the tropical tropopause can be found even a few thousand kilometers away from the convective region. In Fig. 3, we do not differentiate whether divergence is coupled to equatorial waves or not, so any type of convection would be included together for the TIL enhancement with divergent flow. The horizontal structures of sTIL in Fig. 2 can also be shaped by deep convection not related to equatorial waves.

Given the results with divergence from Figures 2 and 3, and the resemblance with the sTIL relationship with relative vorticity in the extratropics, the question arises whether the tropical and extratropical TIL could share the same enhancing mechanism. We postulate an affirmative answer.

The modelling experiments of Wirth (2003, 2004) showed that the stronger TIL in anticyclones in the extratropics was caused by two mechanisms: tropopause lifting and cooling (therefore the higher tropopause with anticyclonic conditions found by Randel et al. (2007); Randel and Wu (2010)); and vertical wind convergence above the anticyclone due to the onset of a secondary circulation between the cyclones and the anticyclones. In the tropics, the tropopause height effect is absent, but there is a clear relationship between sTIL and divergence (Fig. 3a and 3b). Such a horizontally divergent flow is coupled with vertical convergence for continuity reasons. Given that sTIL is rather constant with convergent flow, the TIL enhancement by vertical convergence in the tropics seems to come in hand with the aforementioned hydrostatic adjustment mechanism to deep convective outflow. We propose that vertical wind convergence near the tropopause is one mechanism enhancing the TIL at all latitudes, although caused by different processes: convection in the tropics and baroclinic waves in the extratropics.

Vertical wind convergence is related to anticyclones within baroclinic waves in the extratropics, but tropopause lifting (cooling) and the stratospheric residual circulation also enhance the TIL at the same time (Birner, 2010). In a similar way, we expect that the (100hPa) vertical wind convergence in the tropics is partly related to the equatorial wave spectrum, enhancing the tropical TIL along with other mechanisms (e.g. radiative forcing from water vapor or clouds). The equatorial wave modulation of the tropical TIL is studied in detail in section 4.

3.3 QBO influence

In Fig. 1 we showed that a secondary maximum of N^2 forms within the easterly wind regime of the QBO, just below the zero wind line of the descending westerly QBO phase, giving a double-TIL structure in the vertical N^2 profile in the lowermost stratosphere. This secondary N^2 maximum is responsible for the correlation of enhanced N^2 in the layer 1-3km above the tropopause during the easterly phase of the QBO found by Grise et al. (2010). However, no correlation was found in the layer 0-1km above TP (strictly where the TIL shall be), and no clear difference in TIL strength can be observed (Fig. 1) during the different phases of the QBO. We investigate this in more detail here, looking at the N^2_{max} values found right above the TP instead of averaging over a certain layer.

To define the QBO phase, we take the zonal wind regime in the lowermost stratosphere, nearest to the TIL: around 18-20km altitude, which can be observed in Fig. 1 (black and dashed contour lines). We take two seasons of the same QBO phase in each case from the period between 2007-2013. The easterly phase of the QBO is found in the summers of 2007 and 2012 and the following winters of 2007/08 and 2012/13; while the westerly phase of the QBO is found in winters of 2008/09 and 2010/11 and the following summers of 2009 and 2011.

Figure 4 shows the distribution of N^2_{max} for both winter (left, DJF) and summer (right, JJA). The black lines denote the average distribution over the 2007-2013 period, compared to easterly QBO phase (blue) and westerly QBO (red) as defined in the paragraph above. Winter has a higher mean N^2_{max} ($12.17\times10^{-4}s^{-2}$) than summer ($11.39\times10^{-4}s^{-2}$), in agreement with the results of Grise et al. (2010) and Figures 1 and 3. We find that, during the easterly phase of the QBO (blue lines), the N^2_{max} distributions slightly narrow and shift to lower values, giving lower seasonal means of $12.06\times10^{-4}s^{-2}$ in winter and $10.92\times10^{-4}s^{-2}$ in summer. During the westerly QBO phase (red lines), the opposite happens: the N^2_{max} distributions widen and shift to higher values compared to the average distribution, giving higher seasonal means of $12.74\times10^{-4}s^{-2}$ in winter and $11.49\times10^{-4}s^{-2}$ in summer.

In both winter and summer, the seasonal mean N^2_{max} in the westerly QBO phase is $\sim0.6\times10^{-4}s^{-2}$ higher than during the easterly QBO phase. This difference is highly significant: the standard deviation of the seasonal mean is of the order of $0.02\times10^{-4}s^{-2}$ (each distribution's sample size is ∼20000 profiles), and a t-test (two-tailed distributions with different sample sizes and variances) with these values gives us a t value of ∼20, which is well beyond the 99.9 percent confidence level (critical value ∼3.3).

In summary, from Fig. 4 we conclude that the tropical TIL is stronger during the westerly QBO phase in the lowermost stratosphere. This is not related to changes in the divergence distribution (given the relationship shown in Fig. 3), and is also anticorrelated with the strength of the secondary N^2 maximum found above the TIL region (Fig. 1).

The reason for this behavior of stronger TIL with westerly QBO is probably the modulation by Kelvin waves (the dipole of cooling near the tropopause and warming above), which have a higher activity in the lowermost stratosphere with westerly shear, and a slower vertical propagation (Randel and Wu, 2005) which translates into a longer residence time and longer modulation near the tropopause region to enhance the TIL. How equatorial waves modulate the vertical temperature and N^2 structure is explained below in section 4.

4 Modulation by Equatorial Waves

4.1 Effect on the zonal structure of tropopause height

This section describes how equatorial waves modulate the temperature and N^2 vertical structure in the tropics. As explained in section 2.4, the gridded temperature and N^2 fields are filtered independently with 12 different bandpass filters in the wavenumber-frequency domain. As in Wheeler and Kiladis (1999), no bandpass filters overlap in the wavenumber-frequency domain (see Table 1), and the 12 filters amount for Kelvin waves, equatorial Rossby waves, MJO, and the three modes n = (0,1,2) of westward-propagating (negative wavenumber s) Inertia-Gravity waves (WIG_n), the eastward-propagating ones (positive s, EIG_n), and the zonal wavenumber zero $_{s=0}IG_n$. For each wave type, a daily longitude-height section with its signature on temperature and N^2 is obtained.

Figure 5 shows examples of longitude-height snapshots with the N^2 signature of Kelvin (Fig. 5a), Rossby (Fig. 5b), EIG_n (Fig. 5c) and MJO band (Fig. 5d) at selected dates when the zonal structure of the tropopause (thick black line) is affected by the wave anomalies in an obvious way. In the case of EIG_n the three modes n = (0,1,2) are superimposed: the resulting field is $EIG_n = EIG_0 + EIG_1 + EIG_2$. Note that the filtered N^2 fields include a wide range of wavenumbers, 1-14 in the case of Kelvin waves for example (see Table 1), so the signatures of planetary waves 1 or 2 as well as transient shorter waves (higher wavenumbers) are represented together, giving a patchy appearance sometimes. Nevertheless, clear and coherent structures of the waves' N^2 signatures can be observed in Figure 5.

Temperature perturbations from Kelvin waves were observed to have their maximum near the tropopause in the study by Randel and Wu (2005). In Fig. 5 (with N^2), we see the same for all wave types: their maximum amplitude is generally found near and above the tropopause (black line). Also, zonal variations in tropopause height tend to be aligned with the wave's structure, with N^2 positive anomalies above the tropopause and negative anomalies below. This tropopause adjustment happens where the anomaly's amplitude is large, and is consistent with a dipole of tropopause cooling and warming aloft. This is clearly evident in Fig. 5a within 0-75°E and 100-180°E for Kelvin wave anomalies and in Fig. 5b within 0-125°W and ∼50°E for equatorial Rossby wave anomalies.

Although usually one wave type is dominant (therefore the choosing of separate dates in Fig. 5), different waves can influence the zonal structure of tropopause height at the same time: in Fig. 5 c and d (both of the same day, 2013-08-28), the MJO band creates a zonal variation of tropopause height within 50-125°E, while EIG_n wave anomalies do so within 50-150°W. We note that in most of the cases the strongest wave signatures, as well as zonal variations of the equatorial tropopause, are caused by transient waves with higher wavenumbers (as in every panel in Fig. 5) rather than planetary, quasi-stationary waves 1 or 2.

It is worth highlighting the structures that appear in the MJO band, with large amplitudes near the tropopause. Their eastward propagation, speed and longitudinal location match with the described patterns of deep convection associated to the MJO (Madden and Julian, 1994), but the horizontal and vertical scales are shorter. The N^2 anomalies from Fig. 5d are very similar to the composite temperature anomalies from the MJO band in the study by Kim and Son (2012), who found that MJO temperature anomalies near the tropopause have higher wavenumber due to their longer persistence compared to OLR anomalies.

When daily anomalies without running means are obtained as with our method, we see that the wave's anomalies shape the zonal structure of the tropopause, apart from the tropical tropopause layer (TTL) temperature and N^2 variability.

4.2 Average effect on the seasonal, zonal-mean profile

As explained in section 4.1, Figure 5 shows that the tropopause adjusts to the horizontal and vertical structure of the different wave types, with positive N^2 anomalies tending to be placed right above it. A tropopause-based mean of the wave's signature then should show an average enhancement of the TIL. The contribution of each equatorial wave type to the enhancement of the TIL is shown in Figure 6: for each wave type, a tropopause-based mean of the temperature and N^2 anomalies is done for all longitudes and winter days, achieving the average wave's effect on the seasonal, zonal-mean profile. EIG_n (green), WIG_n (orange) and $_{s=0}IG_n$ (grey) are the sum of all their modes *n* = (0,1,2).

In Fig. 6a, all waves produce a maximum cooling right at the lapse-rate TP and a warming around 1-2km above the tropopause. Our results are in agreement with the study by Grise and Thompson (2013) that showed a cooling effect near the climatological tropopause by equatorial planetary waves, and remind of the dipole with tropopause cooling and lower-stratospheric warming found by Kim and Son (2012) which they attributed to convectively coupled waves. In the study by Kim and Son (2012), Kelvin waves and the MJO were the dominant wave types in short-term TTL temperature variability. By deriving daily fields with no temporal smoothing (see section 2.4.1), we were able to ascertain the role of waves with higher frequencies and zonal wavenumbers than previous studies, pointing out new important features from Fig. 6a: 1) the cooling effect is maximized and centered right at the thermal tropopause, 2) all equatorial wave types give a similar signature, whose magnitude is dependent on the amount of the wave's activity, and 3) the role of transient waves with higher zonal wavenumbers and frequencies is significant: WIG_n, EIG_n and Rossby waves have a bigger impact than the MJO.

The resulting N^2 signature (Fig. 6b) is a maximum N^2 enhancement right above the tropopause, and two regions of destabilization: below the tropopause and 2-3km above it. The overall effect is a TIL enhancement tightly close to the thermal tropopause. In Fig. 5 we showed obvious examples of tropopause adjustment to the wave structure with positive N^2 anomalies right above the tropopause. Given that the signature in the seasonal zonal-mean profile is considerable in Fig. 6, it can be concluded that the tropopause adjustment to the different waves (and the resulting dipole of tropopause cooling / warming above) occurs continuously, but not always so clearly as in Fig. 5. We stress that the signatures seen in Figures 5 and 6 were obtained by filtering the temperature and N^2 fields directly and independently, without any filtering in the vertical dimension.

Looking at the different wave types separately in Fig.6, the Kelvin wave (blue) has the strongest temperature signature (Fig. 6a), but owing to its longer vertical scale (see Fig. 5a) the temperature gradient that the Kelvin wave produces is closer to the rest of the waves', giving an average N^2 enhancement of $0.35\times10^{-4}s^{-2}$/day. The signatures of EIG_n (green), WIG_n (orange) and Rossby (red) waves give an average TIL enhancement of $\sim0.25\times10^{-4}s^{-2}$/day each, followed by the MJO band (purple, $0.1\times10^{-4}s^{-2}$/day). The $_{s=0}IG_n$ wave type (grey), although lacking zonal structures by definition and having little activity, still gives a minor TIL enhancement. The relative N^2 minima below the tropopause and above the TIL region in the seasonal zonal-mean profile (e.g. Grise et al. (2010)) can be attributed to the equatorial wave modulation as well.

The total effect of the equatorial waves on the equatorial zonal-mean seasonal temperature profile is a $\sim$1.1K/day cooling of the tropopause and a $\sim$0.5K/day warming above, with a resulting TIL enhancement of $\sim1.2\times10^{-4}s^{-2}$/day. Fig. 6 shows the mean wave effect during winter; the results are similar during summer (see Appendix B, figure B1) except for a slightly weaker effect of the MJO band, given its lower average activity in that season.

We acknowledge the possibility that the wave signals shown in Figs. 5 and 6 may not be 100% dynamical: a radiative component is included if clouds are present near the tropopause (radiative cooling at the cloud top that creates a temperature inversion). Part of the equatorial wave spectrum in the TTL is known to be coupled with convection, a small part of which reaches the tropopause (Wheeler and Kiladis, 1999; Fueglistaler et al., 2009), and the occurrence of cirrus clouds is also related to equatorial waves (Virts and Wallace, 2010). Case studies using GPS-RO data have investigated the temperature inversion generally found at cloud tops, for convective clouds (Biondi et al., 2012) and non-convective cirrus clouds (Taylor et al., 2011). The signal from any cloud coupled with an equatorial wave would be captured by its corresponding wavenumber-frequency domain filter, since the cloud signal would travel together with the wave in the same domain. Therefore a part of the mean wave signal shown in Fig. 6 could be due to the temperature inversion of (wave-coupled) cloud-tops near the tropopause, but quantifying this is beyond the scope of our study. Nevertheless, it is logical to assume that the radiative part associated to the equatorial wave signal shall be small, since equatorial waves are not radiatively driven and their propagation is explained by dry dynamics.

Our results from this section (Figs. 5 and 6) agree with earlier studies that derived equatorial wave anomalies from GPS-RO data (the Kelvin and MJO signatures and their amplification near the tropopause (Randel and Wu, 2005; Kim and Son, 2012)). Also, Fig. 6 confirms the effect of equatorial waves on the mean temperature profile (tropopause cooling and warming above forming a dipole (Kim and Son, 2012; Grise and Thompson, 2013)) and their crucial role in enhancing the TIL in the tropics (Grise et al., 2010). The novelty in our study resides in that we include small-scale, higher-frequency waves (e.g. Inertia-Gravity waves); and that we are able to quantify the effect of each equatorial wave type separately by tropopause-based averaging of the filtered wave anomalies.

Our results from this section should not be viewed as a mere quantification of the waves themselves or an artifact of the tropopause-coordinate. Although transient and instantaneous, there are motions associated to the wave signals that locally lift/cool/modulate the tropopause, and also warm the air aloft. Another characteristic of the waves is that they amplify next to and above the tropopause (Fig. 5), and also increase their vertical tilt (Fig. 5a, visible for Kelvin waves), which increases the wave signal in the TIL region, and also increases the area of positive N^2 anomaly above the tropopause. This is a response of the wave to the elevated N^2 values in the lowermost stratosphere, in agreement with linear theory, which in turn enhances the TIL further, working as a positive feedback. Although our results point in this direction, more research needs to be carried out to consider such a feedback as a robust feature of the global tropopause region.

4.3 TIL without equatorial wave signals

Figure 7 shows the daily evolution of the equatorial zonal-mean, tropopause-based N^2 profile (Fig. 7a), and the resulting N^2 profile when the equatorial wave signals are subtracted (Fig. 7b). The display is very similar to that of Fig. 1, but in order to allow the subtraction of the equatorial wave signal, for Fig. 7 we use the gridded dataset obtained in section 2.4, from COSMIC profiles only (2007-2013) and 10°S-10°N without any temporal smoothing of N^2.

A clear difference in the TIL region can be observed in Fig. 7b: without the equatorial wave signal, the TIL in the first kilometer above the tropopause is much weakened, from N^2 values of 7-9$\times10^{-4}s^{-2}$ right above the tropopause (orange-red colors in Fig. 7a) to values of 6-7$\times10^{-4}s^{-2}$ (yellow-orange colors in Fig. 7b) and even less sometimes. In Fig. 7b, the stronger TIL with N^2 values above 7$\times10^{-4}s^{-2}$ (red) is very sparse in time and restricted to wintertime. The differences between Fig. 7a and Fig. 7b agree well with the magnitude of mean TIL enhancement calculated in section 4.2 (Fig. 6).

However, in Fig. 7b the deeper N^2 structures between the tropopause and ∼20km altitude remain intact, as well as the secondary N^2 maximum below the descending westerly QBO phase: they are basically the same as in Fig. 7a and therefore not directly modulated by equatorial waves.

What other mechanisms could enhance the TIL in the tropics? Deep convection that is not coupled with any equatorial wave can also lead to tropopause cooling (by hydrostatic adjustment) and TIL enhancement, as discussed in section 3.2 (Holloway and Neelin, 2007; Paulik and Birner, 2012). Given that deep convection near the equator is more frequent in winter, this would explain the occurrence of stronger TIL in Fig. 7b within this season. Radiative cooling from non-convective cloud tops near the tropopause (e.g. Taylor et al. (2011)), or from strong humidity gradients across the tropopause, can also enhance the gradients that lead to TIL enhancement.

Also note that the wave signals in Fig. 5, their average signature in Fig. 6, and the subtracted signals in Fig. 7b, all come from the instantaneous filtered anomalies: once the wave has left the tropopause region, or dissipated, our filters do not capture any signal that could modulate the TIL. The wave-mean flow interaction is not visible with our method, since its more persistent temperature and N^2 effect would not travel in the wavenumber-frequency domain any more.

The secondary N^2 maximum below the descending westerly QBO phase can be related to the temperature anomaly associated to the wind shear of the QBO (Baldwin et al., 2001), which affects the background N^2 structure throughout the stratosphere. It can be seen in Figs. 1 and 7 that during the easterly phase of the QBO, N^2 between 20-30km altitude is generally higher than within westerlies. It is also possible that the N^2 maximum right below the zero wind line of the descending westerly QBO could be forced by a temperature anomaly from the dissipation of Kelvin waves, which propagate vertically with easterlies until they reach westerly shear. In this case, it would be an indirect effect of Kelvin waves: once they dissipate there is no signal to be captured by our filter. Quantifying this effect (for both the secondary N^2 maximum and the TIL, as in the previous paragraph) is beyond the scope of our study.

5 Discussion: Applicability of the Wave Modulation in the Extratropics

As Fig. 6 showed, all equatorial wave types have the same effect on the temperature and N^2 seasonal zonal-mean vertical profiles, only varying in magnitude. Since all wave types have the same signature, one could expect a similar picture coming from the extratropical wave spectrum. Taking the extratropical baroclinic Rossby wave as an example: the embedded cyclones-anticyclones with lower-higher tropopause would be an example of tropopause adjustment to the anomalies associated with the wave, as in Fig. 5. Given that the zonal variability of TP_z at mid-latitudes is much larger than within the tropics (3km against 0.8km, see Appendix A) and that temperature gradients next to the jet stream are also of much higher magnitude, it is probable that the extratropical Rossby wave's N^2 signature on the mid-latitude zonal mean profile is even stronger than the signal observed from Kelvin waves in Fig. 6, which dominates in the tropics. Inertia-gravity waves are also widely present in the extratropics. Depending on the amplitude they reach next to the extratropical tropopause, this wave type shall also contribute to enhance the TIL, which is predicted by the modelling experiment by Kunkel et al. (2014).

The wavenumber-frequency domain filtering method used with the dispersion curves of extratropical wave modes would be suited to quantify the modulation of each wave mode on the extratropical TIL, in the same way our study has done with equatorial waves. Also, similarly to section 4.3 and Fig. 7, it could be possible to show how much of the TIL in the extratropics is due to processes other than the instantaneous modulation by extratropical waves (i.e. radiative forcing or residual circulation). Preliminary results show that the method used in this paper is indeed applicable in the extratropics as well, and a new paper about this is in preparation.

6 Concluding Remarks

Our study explores the horizontal and vertical variability of the tropical TIL, the effect of the QBO, the role of near-tropopause divergence and the role of equatorial waves in enhancing the tropical TIL. Overall it gives an in-depth observational description of the TIL properties in the tropics and the mechanisms that lead to its enhancement in a region where research has focused very little so far.

Our results agree with the seasonality and location of the tropical TIL described by Grise et al. (2010), with stronger TIL centered at the equator and peaking during NH winter. We describe a new feature: a secondary N^2 maximum that forms above the TIL region within the easterly wind regime of the QBO, below the zero wind line of the descending westerly QBO (Fig. 1). This secondary maximum leads to a double-TIL-like structure in the stability profile, and explains the correlation of enhanced N^2 in the 1-3km layer above the tropopause with easterly QBO found by Grise et al. (2010). The behavior of the secondary N^2 maximum is anticorrelated with the TIL strength (strictly the N^2_{max} found less than 1km above the tropopause): the TIL is stronger during the westerly phase of the QBO in the lowermost stratosphere (Fig. 4).

The zonal structure of the tropical TIL shows a stronger (weaker) TIL with near-tropopause divergent (convergent) flow (Fig. 2). This sTIL-divergence relationship (Fig. 3) is analogous to that of TIL strength with relative vorticity found in the extratropics (Randel et al., 2007; Randel and Wu, 2010; Pilch Kedzierski et al., 2015), and we suggest that vertical wind convergence is a TIL enhancing mechanism that the tropics (divergent flow) and extratropics (anticyclones) have in common.

We also quantified the signature of the different equatorial waves on the seasonal zonal-mean temperature and N^2 profile (Fig. 6). All wave types have a maximum cooling effect at the thermal tropopause, and a warming effect above, enhancing the TIL strength very close to the tropopause. The way this modulation is done is by tropopause adjustment to the vertical structure of the wave's associated anomalies when these have high amplitudes (Fig. 5). While agreeing with earlier studies that used GPS-RO to investigate equatorial waves (Randel and Wu, 2005; Kim and Son, 2012), our results show the importance of small-scale, high-frequency waves due to our method with minimized temporal smoothing, which enables us to quantify and compare the role of each different equatorial wave type for the first time. Inertia-gravity and Rossby waves play a very significant role, with a bigger signature than the MJO, and Kelvin waves dominate the tropopause cooling, warming above and the resulting TIL enhancement (Fig. 6).

Without the equatorial wave signal, the TIL is much weakened (Fig. 7) but part of it remains, and we point to non-wave-coupled deep convection (tropopause cooling by hydrostatic adjustment, (Holloway and Neelin, 2007; Paulik and Birner, 2012)) and radiative effects from clouds or humidity gradients as other possible mechanisms that could enhance the tropical TIL.

We suggest that this wave modulation will also be present in the extratropics with baroclinic Rossby and inertia-gravity waves as main contributors, which will be the subject of a follow-on study.

Appendix A: Divergence vs Tropopause Height

Figure A1 shows divergence versus tropopause height (TP_z) diagrams, as in Fig. 3 with TIL strength (section 3.2). There is no clear link between a higher tropopause and a stronger TIL. In summer (Fig. A1 a), the relation of higher TP_z with divergent flow is very small: the difference between convergent-divergent flow is only of 0.8km, while the difference in cyclones-anticyclones in the extratropics is over 3km (Randel and Wu, 2010). In winter (Fig. A1 b) this relation is non-existent: the tropical TP_z is around 17km at all divergence-convergence values.

Appendix B: Equatorial Wave Modulation in Summer

Figure B1 is the summer counterpart of Fig. 6 from section 4. The average effect of each wave in summer (Fig. B1) is very similar to the one from winter (Fig. 6), except for a smaller MJO signature.

Appendix C: Caveat on the Filtering of Periods of 1-2 Days from a Daily Dataset

As showed in Table 1, the modes $n = 2$ of all inertia-gravity wave types (EIG_n, WIG_n and $_{s=0}IG_n$) are defined for periods between 1-2 days. With a dataset of daily temporal resolution, filtering with such periods has to be taken with lots of caution for two reasons:

1) Oscillations with periods below 2 times the temporal resolution of the dataset (below 2 days in this case) are underestimated (best case scenario), or not resolved at all by the dataset. Nevertheless we applied these filters, should any part of the wave signal be discernible.

2) Once filtered, the resulting wave anomalies are subject to include spurious signals because of spectral ringing. It is very important to know how much of the wave signature in Figure 6 comes from this artifact, since all modes n = (0,1,2) are summed-up there.

We computed the mean signature of modes n = (0,1,2) separately, and found that all of the signal in Fig. 6 comes from modes n = 0 and 1. This means that the filters of inertia-gravity waves with periods between 1-2 days do not capture any signal at all (artificial or not), and therefore make no contribution to our results. The equatorial wave signature in Fig. 6 (and Fig. B1) comes entirely from oscillations that are resolved by our gridded daily dataset obtained from COSMIC GPS-RO profiles.

Waves with periods below 2 days could modulate the tropical tropopause region and the TIL, though: only the current amount of GPS-RO profiles is not enough to resolve this. It shall be possible to do so once COSMIC-2 profiles (a much increased amount compared to current data) are available.

Acknowledgements. This study was completed within the Helmholtz-University Young Investigators Group NATHAN project, funded by the Helmholtz Association through the president's Initiative and Networking Fund and the GEOMAR Helmholtz-Centre for Ocean Research in Kiel. We thank the ECMWF data server for the freely available ERA-Interim data; and UCAR for the COSMIC, CHAMP and GRACE satellite missions' temperature profiles. Comments by Joowan Kim and two anonymous reviewers are highly appreciated and clearly helped to improve the manuscript significantly. The assistance accessing different datasets and discussions with Sandro Lubis, Wuke Wang and Sebastian Wahl are also appreciated.

References

Anthes, R. A., Bernhardt, P. A., Chen, Y., Cucurull, L., Dymond, K. F., Ector, D., Healy, S. B., Ho, S.-P., Hunt, D. C., Kuo, Y.-H., Liu, H., Manning, K., McCormick, C., Meehan, T. K., Randel, W. J., Rocken, C., Schreiner, W. S., Sokolovskiy, S. V., Syndergaard, S., Thompson, D. C., Trenberth, K. E., Wee, T.-K., Yen, N. L., and Zeng, Z.: The COSMIC/FORMOSAT-3 Mission: Early Results, Bulletin of the American Meteorological Society, 89, 313, doi:10.1175/BAMS-89-3-313, 2008.

Baldwin, M. P., Gray, L. J., Dunkerton, T. J., Hamilton, K., Haynes, P. H., Randel, W. J., Holton, J. R., Alexander, M. J., Hirota, I., Horinouchi, T., Jones, D. B. A., Kinnersley, J. S., Marquardt, C., Sato, K., and Takahashi, M.: The quasi-biennial oscillation, Reviews of Geophysics, 39, 179–229, doi:10.1029/1999RG000073, 2001.

Bell, S. W. and Geller, M. A.: Tropopause inversion layer: Seasonal and latitudinal variations and representation in standard radiosonde data and global models, Journal of Geophysical Research (Atmospheres), 113, D05109, doi:10.1029/2007JD009022, 2008.

Beyerle, G., Schmidt, T., Michalak, G., Heise, S., Wickert, J., and Reigber, C.: GPS radio occultation with GRACE: Atmospheric profiling utilizing the zero difference technique, Geophysical Research Letters, 32, L13806, doi:10.1029/2005GL023109, 2005.

Biondi, R., Randel, W. J., Ho, S.-P., Neubert, T., and Syndergaard, S.: Thermal structure of intense convective clouds derived from GPS radio occultations, Atmospheric Chemistry & Physics, 12, 5309–5318, doi:10.5194/acp-12-5309-2012, 2012.

Birner, T.: Fine-scale structure of the extratropical tropopause region, Journal of Geophysical Research (Atmospheres), 111, D04104, doi:10.1029/2005JD006301, 2006.

Birner, T.: Residual Circulation and Tropopause Structure, Journal of Atmospheric Sciences, 67, 2582–2600, doi:10.1175/2010JAS3287.1, 2010.

Birner, T., Dörnbrack, A., and Schumann, U.: How sharp is the tropopause at midlatitudes?, Geophysical Research Letters, 29, 1700, doi:10.1029/2002GL015142, 2002.

Birner, T., Sankey, D., and Shepherd, T. G.: The tropopause inversion layer in models and analyses, Geophysical Research Letters, 33, L14804, doi:10.1029/2006GL026549, 2006.

Dee, D. P., Uppala, S. M., Simmons, A. J., Berrisford, P., Poli, P., Kobayashi, S., Andrae, U., Balmaseda, M. A., Balsamo, G., Bauer, P., Bechtold, P., Beljaars, A. C. M., van de Berg, L., Bidlot, J., Bormann, N., Delsol, C., Dragani, R., Fuentes, M., Geer, A. J., Haimberger, L., Healy, S. B., Hersbach, H., Hólm, E. V., Isaksen, L., Kållberg, P., Köhler, M., Matricardi, M., McNally, A. P., Monge-Sanz, B. M., Morcrette, J.-J., Park, B.-K., Peubey, C., de Rosnay, P., Tavolato, C., Thépaut, J.-N., and Vitart, F.: The ERA-Interim reanalysis: configuration and performance of the data assimilation system, Quarterly Journal of the Royal Meteorological Society, 137, 553–597, doi:10.1002/qj.828, 2011.

Erler, A. R. and Wirth, V.: The Static Stability of the Tropopause Region in Adiabatic Baroclinic Life Cycle Experiments, Journal of Atmospheric Sciences, 68, 1178–1193, doi:10.1175/2010JAS3694.1, 2011.

Fueglistaler, S., Dessler, A. E., Dunkerton, T. J., Folkins, I., Fu, Q., and Mote, P. W.: Tropical tropopause layer, Reviews of Geophysics, 47, RG1004, doi:10.1029/2008RG000267, 2009.

Gettelman, A. and Birner, T.: Insights into Tropical Tropopause Layer processes using global models, Journal of Geophysical Research (Atmospheres), 112, D23104, doi:10.1029/2007JD008945, 2007.

Gettelman, A., Hoor, P., Pan, L. L., Randel, W. J., Hegglin, M. I., and Birner, T.: The Extratropical Upper Troposphere and Lower Stratosphere, Reviews of Geophysics, 49, RG3003, doi:10.1029/2011RG000355, 2011.

Grise, K. M. and Thompson, D. W. J.: On the Signatures of Equatorial and Extratropical Wave Forcing in Tropical Tropopause Layer Temperatures, Journal of Atmospheric Sciences, 70, 1084–1102, doi:10.1175/JAS-D-12-0163.1, 2013.

Grise, K. M., Thompson, D. W. J., and Birner, T.: A Global Survey of Static Stability in the Stratosphere and Upper Troposphere, Journal of Climate, 23, 2275–2292, doi:10.1175/2009JCLI3369.1, 2010.

Hegglin, M. I., Boone, C. D., Manney, G. L., and Walker, K. A.: A global view of the extratropical tropopause transition layer from Atmospheric Chemistry Experiment Fourier Transform Spectrometer O_3, H_2O, and CO, Journal of Geophysical Research (Atmospheres), 114, D00B11, doi:10.1029/2008JD009984, 2009.

Holloway, C. E. and Neelin, J. D.: The Convective Cold Top and Quasi Equilibrium*, Journal of Atmospheric Sciences, 64, 1467, doi:10.1175/JAS3907.1, 2007.

Kim, J. and Son, S.-W.: Tropical Cold-Point Tropopause: Climatology, Seasonal Cycle, and Intraseasonal Variability Derived from COSMIC GPS Radio Occultation Measurements, Journal of Climate, 25, 5343–5360, doi:10.1175/JCLI-D-11-00554.1, 2012.

Kunkel, D., Hoor, P., and Wirth, V.: Can inertia-gravity waves persistently alter the tropopause inversion layer?, Geophysical Research Letters, 41, 7822–7829, doi:10.1002/2014GL061970, 2014.

Kunz, A., Konopka, P., Müller, R., Pan, L. L., Schiller, C., and Rohrer, F.: High static stability in the mixing layer above the extratropical tropopause, Journal of Geophysical Research (Atmospheres), 114, D16305, doi:10.1029/2009JD011840, 2009.

Lindzen, R. D.: Planetary Waves on Beta-Planes, Monthly Weather Review, pp. 441–451, 1967.

Madden, R. A. and Julian, P. R.: Observations of the 40 50-Day Tropical Oscillation - A Review, Monthly Weather Review, 122, 814, doi:10.1175/1520-0493(1994)122<0814:OOTDTO>2.0.CO;2, 1994.

Matsuno, T.: Quasi-Geostrophic Motions in the Equatorial Area, Journal of the Meteorological Society of Japan. Ser. II, 44, 25–43, 1966.

Miyazaki, K., Watanabe, S., Kawatani, Y., Sato, K., Tomikawa, Y., and Takahashi, M.: Transport and Mixing in the Extratropical Tropopause Region in a High-Vertical-Resolution GCM. Part II: Relative Importance of Large-Scale and Small-Scale Dynamics, Journal of Atmospheric Sciences, 67, 1315–1336, doi:10.1175/2009JAS3334.1, 2010a.

Miyazaki, K., Watanabe, S., Kawatani, Y., Tomikawa, Y., Takahashi, M., and Sato, K.: Transport and Mixing in the Extratropical Tropopause Region in a High-Vertical-Resolution GCM. Part I: Potential Vorticity and Heat Budget Analysis, Journal of Atmospheric Sciences, 67, 1293–1314, doi:10.1175/2009JAS3221.1, 2010b.

Paulik, L. C. and Birner, T.: Quantifying the deep convective temperature signal within the tropical tropopause layer (TTL), Atmospheric Chemistry & Physics, 12, 12 183–12 195, doi:10.5194/acp-12-12183-2012, 2012.

Pilch Kedzierski, R., Matthes, K., and Bumke, K.: Synoptic-scale behavior of the extratropical tropopause inversion layer, Geophysical Research Letters, 42, 10,018–10,026, doi:10.1002/2015GL066409, 2015GL066409, 2015.

Poli, P., Healy, S. B., and Dee, D. P.: Assimilation of Global Positioning System radio occultation data in the ECMWF ERA-Interim reanalysis, Quarterly Journal of the Royal Meteorological Society, 136, 1972–1990, doi:10.1002/qj.722, 2010.

Randel, W. J. and Wu, F.: Kelvin wave variability near the equatorial tropopause observed in GPS radio occultation measurements, Journal of Geophysical Research (Atmospheres), 110, D03102, doi:10.1029/2004JD005006, 2005.

Randel, W. J. and Wu, F.: The Polar Summer Tropopause Inversion Layer, Journal of Atmospheric Sciences, 67, 2572–2581, doi:10.1175/2010JAS3430.1, 2010.

Randel, W. J., Wu, F., and Forster, P.: The Extratropical Tropopause Inversion Layer: Global Observations with GPS Data, and a Radiative Forcing Mechanism, Journal of Atmospheric Sciences, 64, 4489, doi:10.1175/2007JAS2412.1, 2007.

Schmidt, T., Cammas, J.-P., Smit, H. G. J., Heise, S., Wickert, J., and Haser, A.: Observational characteristics of the tropopause inversion layer derived from CHAMP/GRACE radio occultations and MOZAIC aircraft data, Journal of Geophysical Research (Atmospheres), 115, D24304, doi:10.1029/2010JD014284, 2010.

Schreck, C.: Extract equatorial waves by filtering in the Wheeler-Kiladis wavenumber-frequency domain., https://www.ncl.ucar.edu/Document/Functions/User_contributed/kf_filter.shtml, 2009.

Son, S.-W. and Polvani, L. M.: Dynamical formation of an extra-tropical tropopause inversion layer in a relatively simple general circulation model, Geophysical Research Letters, 34, L17806, doi:10.1029/2007GL030564, 2007.

Son, S.-W., Tandon, N. F., and Polvani, L. M.: The fine-scale structure of the global tropopause derived from COSMIC GPS radio occultation measurements, Journal of Geophysical Research (Atmospheres), 116, D20113, doi:10.1029/2011JD016030, 2011.

Taylor, J. R., Randel, W. J., and Jensen, E. J.: Cirrus cloud-temperature interactions in the tropical tropopause layer: a case study, Atmospheric Chemistry & Physics, 11, 10 085–10 095, doi:10.5194/acp-11-10085-2011, 2011.

Virts, K. S. and Wallace, J. M.: Annual, Interannual, and Intraseasonal Variability of Tropical Tropopause Transition Layer Cirrus, Journal of Atmospheric Sciences, 67, 3097–3112, doi:10.1175/2010JAS3413.1, 2010.

Wang, W., Matthes, K., Schmidt, T., and Neef, L.: Recent variability of the tropical tropopause inversion layer, Geophysical Research Letters, 40, 6308–6313, doi:10.1002/2013GL058350, 2013.

Wheeler, M. and Kiladis, G. N.: Convectively Coupled Equatorial Waves: Analysis of Clouds and Temperature in the Wavenumber-Frequency Domain., Journal of Atmospheric Sciences, 56, 374–399, doi:10.1175/1520-0469(1999)056<0374:CCEWAO>2.0.CO;2, 1999.

Wickert, J., Reigber, C., Beyerle, G., König, R., Marquardt, C., Schmidt, T., Grunwaldt, L., Galas, R., Meehan, T. K., Melbourne, W. G., and Hocke, K.: Atmosphere sounding by GPS radio occultation: First results from CHAMP, Geophysical Research Letters, 28, 3263–3266, doi:10.1029/2001GL013117, 2001.

Wirth, V.: Static Stability in the Extratropical Tropopause Region., Journal of Atmospheric Sciences, 60, 1395–1409, doi:10.1175/1520-0469(2003)060<1395:SSITET>2.0.CO;2, 2003.

Wirth, V.: A dynamical mechanism for tropopause sharpening, Meteorologische Zeitschrift, 13, 477–484, doi:10.1127/0941-2948/2004/0013-0477, 2004.

Wirth, V. and Szabo, T.: Sharpness of the extratropical tropopause in baroclinic life cycle experiments, Geophysical Research Letters, 34, 2809, doi:10.1029/2006GL028369, 2007.

WMO: Meteorology-A three-dimensional science, WMO Bull., 6, 134–138, 1957.

Yulaeva, E., Holton, J. R., and Wallace, J. M.: On the Cause of the Annual Cycle in Tropical Lower-Stratospheric Temperatures., Journal of Atmospheric Sciences, 51, 169–174, doi:10.1175/1520-0469(1994)051<0169:OTCOTA>2.0.CO;2, 1994.

Table 1. Parameters used to bound the filter of the different equatorial wave types, with the meridional mode *n* as subscript: *t* (period, in days), *s* (zonal planetary wavenumber) and *h* (equivalent depth, in m)

Wave type	t_{min}	t_{max}	s_{min}	s_{max}	h_{min}	h_{max}
Eq. Rossby	6	70	-14	-1	6	600
Kelvin	4	30	1	14	6	600
MJO	30	96	2	5	8	90
WIG_0	2.5	6	-10	-1	6	360
WIG_1	2	2.5	-15	-1	8	90
WIG_2	1	2	-15	-1	8	90
EIG_0	2.5	4	1	15	8	90
EIG_1	2	2.5	1	15	8	90
EIG_2	1	2	1	15	8	90
${}_{s=0}IG_0$	3	6	-0.1	0.1	8	90
${}_{s=0}IG_1$	2	3	-0.1	0.1	8	90
${}_{s=0}IG_2$	1	2	-0.1	0.1	8	90

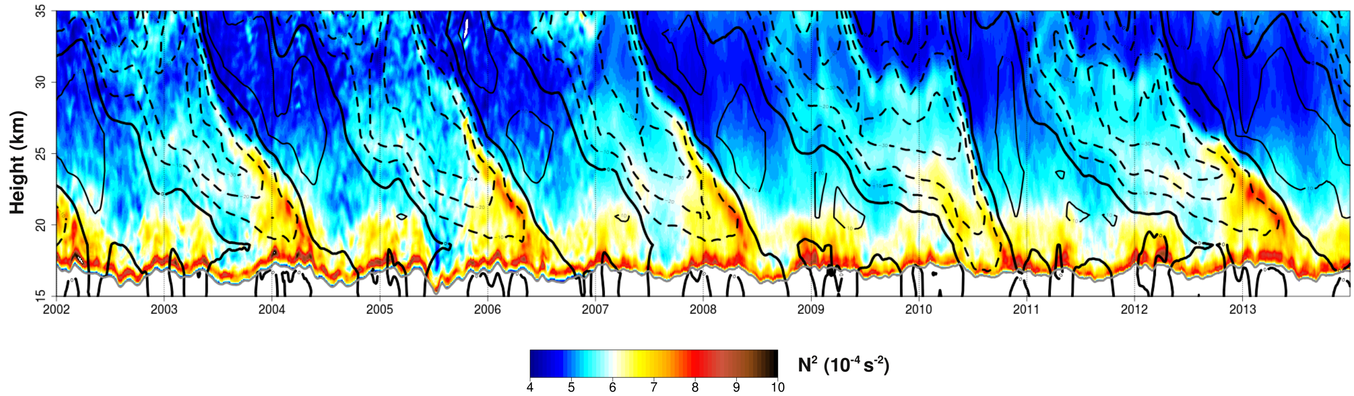

Figure 1. Daily evolution of the tropopause-based, equatorial (5°S-5°N) zonal mean N^2 vertical profile between 2002-2013 (colors). 2002-2006 from CHAMP+GRACE GPS-RO profiles, 2007-2013 from COSMIC. The grey line denotes the tropopause height (TP_z). Thin black contours denote positive (westerly) mean zonal wind, with a thicker contour for the zero line, dashed contours for negative (easterly) winds, and a 10m/s separation. To improve visibility, each day shows the running mean N^2 profile and TP_z of +-7 days. In the case of the winds, the running mean is made for +-15 days.

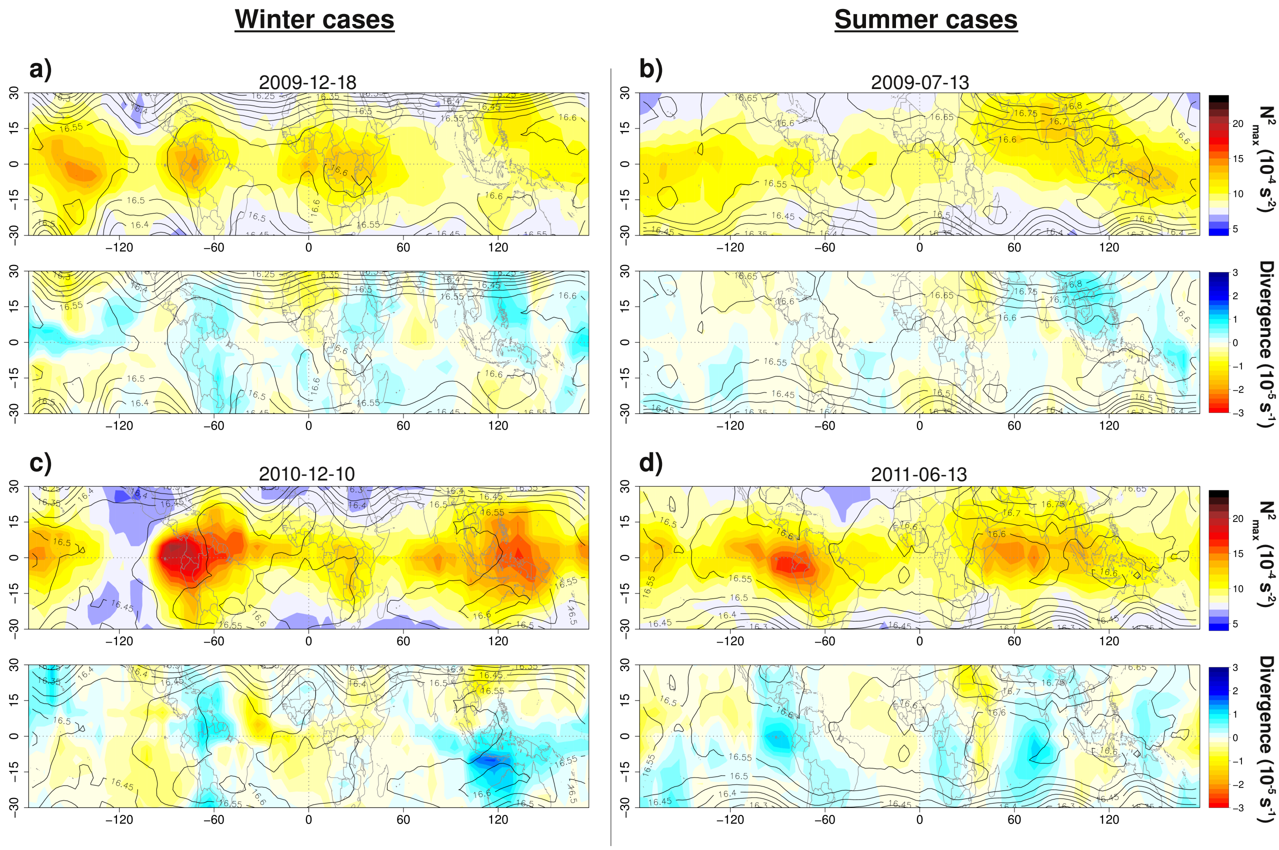

Figure 2. Maps of daily TIL strength (N^2_{max}, first and third rows) and 100hPa divergence (second and fourth rows). Winter cases are on the left side, and summer cases are on the right side. Corresponding color scales are on the right end. Contour lines show the 100hPa geopotential height (in km' with 50m' interval).

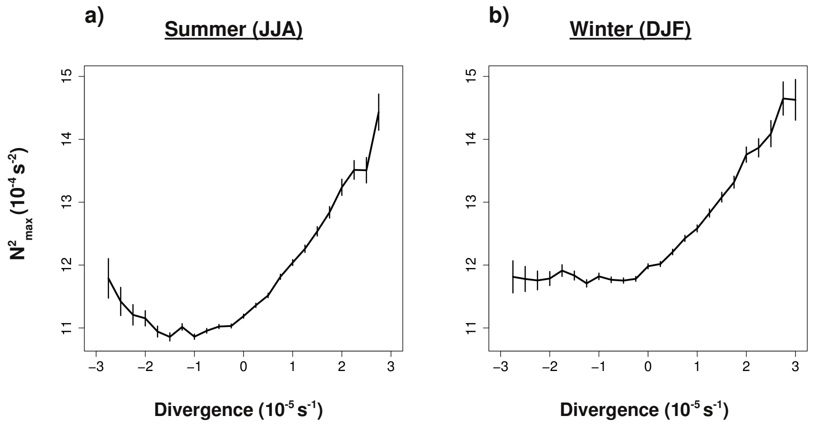

Figure 3. Diagrams of divergence versus TIL strength (N^2_{max}) for the latitude band 10°S-10°N. a) belongs to the summer season (JJA), and b) to the winter season (DJF). Vertical bars denote one standard deviation of the mean value.

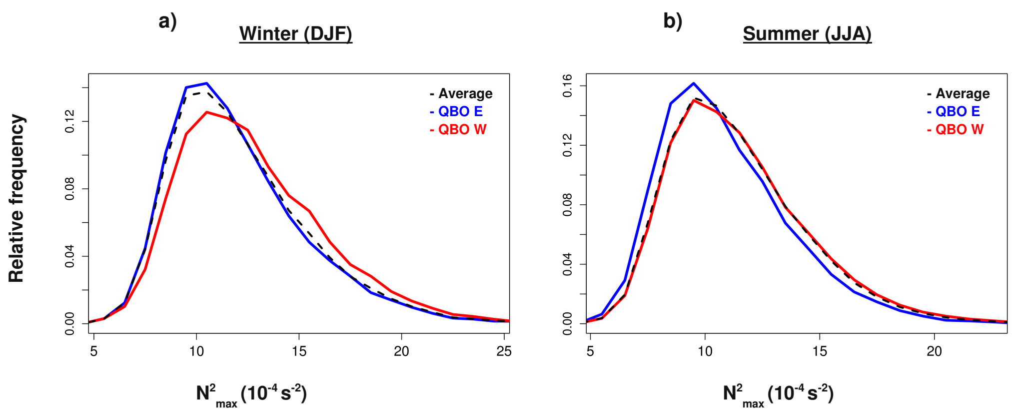

Figure 4. Histograms with relative frequency of TIL strength (N^2_{max}), for winter (a, DJF) and summer (b, JJA). The black dashed line denotes the average seasonal distribution. The blue line shows distributions during the easterly phase of the QBO in the lowermost stratosphere, and the red line shows the distributions during the westerly QBO phase.

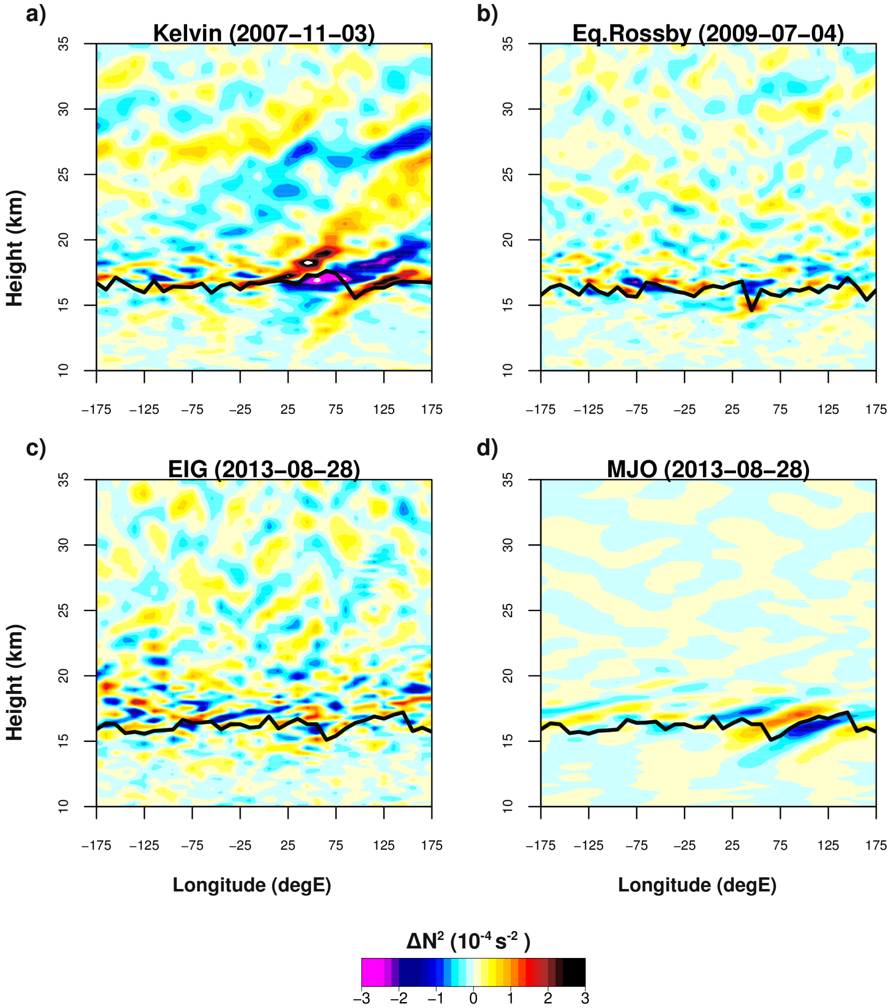

Figure 5. Longitude-height snapshots of the N^2 signature of different wave types at certain dates: a) Kelvin wave, b) Rossby wave, c) Eastward IGW (EIG_n), d) MJO band. The black line denotes the thermal tropopause.

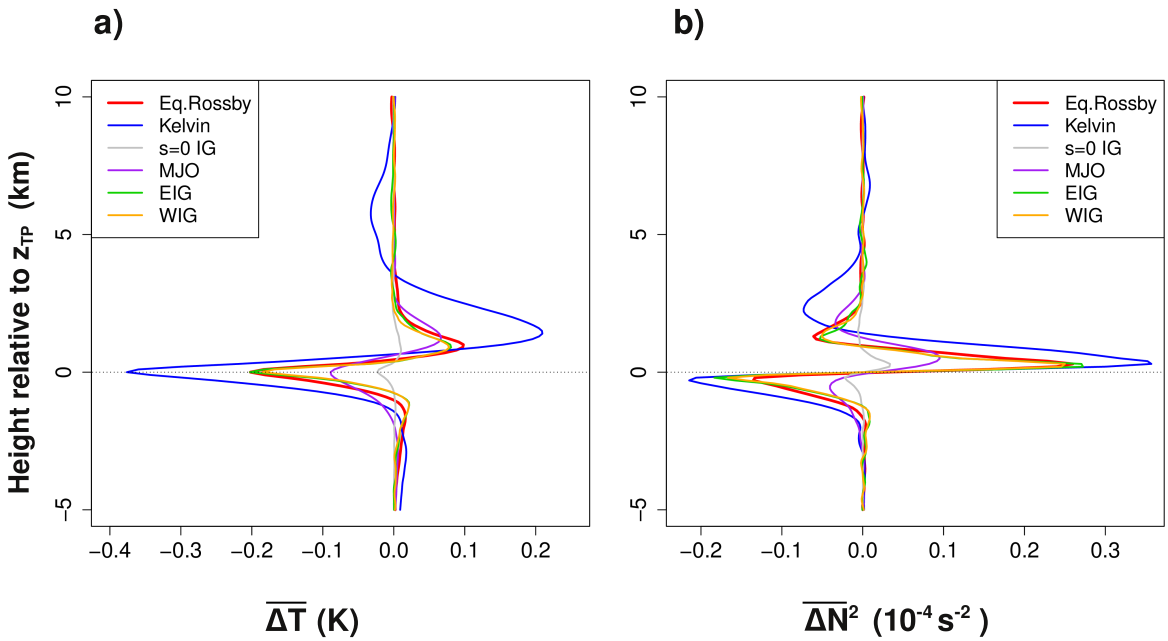

Figure 6. Winter (DJF) average signature of the different wave types, as the mean anomaly of (a) temperature and (b) N^2 in the equatorial zonal-mean vertical profiles (10°S-10°N).

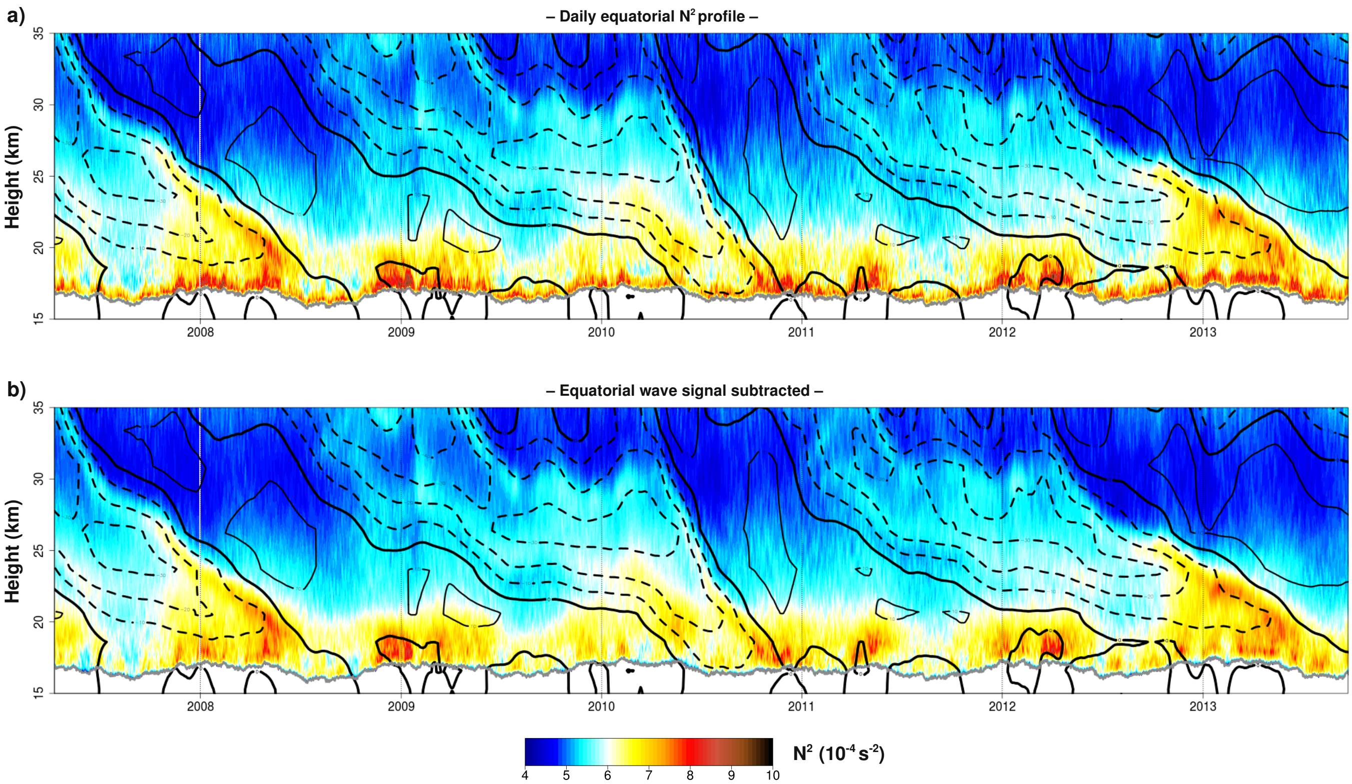

Figure 7. a) Daily evolution of the tropopause-based, equatorial (10°S-10°N) zonal mean N^2 vertical profile between 2007-2013 (colors) from COSMIC GPS-RO profiles. The grey line denotes the tropopause height (TP_z). Thin black contours denote positive (westerly) mean zonal wind, with a thicker contour for the zero line, dashed contours for negative (easterly) winds, and a 10m/s separation. To improve visibility, the winds are displayed with a running mean of +-15 days. No running mean is applied to the N^2 vertical profile or TP_z in order to allow the subtraction of the equatorial wave signal. b) Equatorial wave signal subtracted from the N^2 vertical profile.

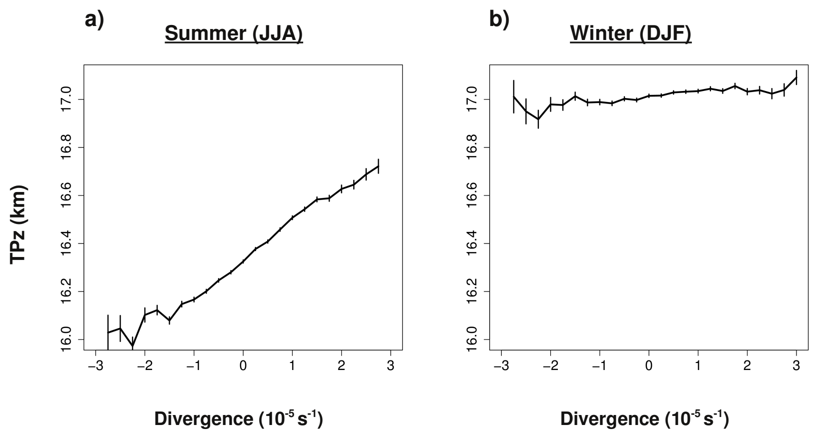

Figure A1. Diagrams of divergence versus tropopause height (TP_z, km) for the latitude band 10°S-10°N. a) belongs to the summer season (JJA), and b) to the winter season (DJF). Vertical bars denote one standard deviation of the mean value.

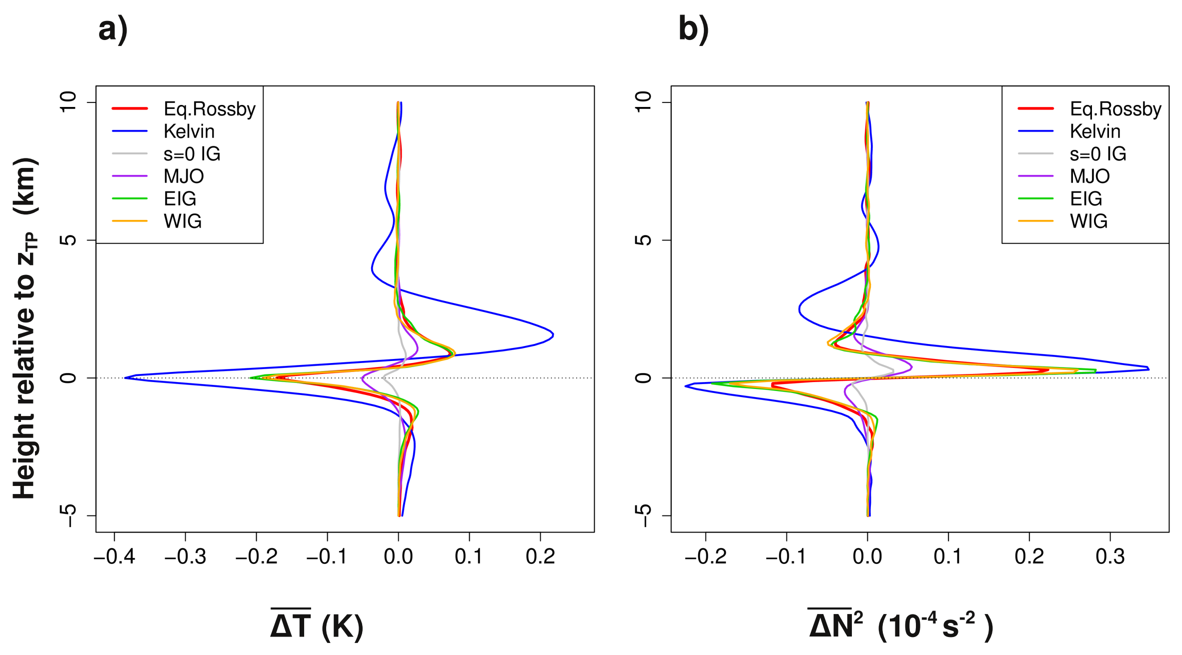

Figure B1. Summer (JJA) average signature of the different wave types, as the mean anomaly of (a) temperature and (b) N^2 in the equatorial zonal-mean vertical profiles (10°S-10°N).